

METALS DEPOSITION IN NORTHERN ARIZONA RESERVOIRS

Draft Final Report

March 24, 2005



Submitted to:

Amanda Fawley

Arizona Department of Environmental Quality

1110 W. Washington St.

Phoenix, Arizona 85007

Submitted by:

Paul T. Gremillion and Jaime L. Toney

Northern Arizona University

Flagstaff, Arizona 86001

Table of Contents

Section	Page
Table of Contents	i
List of Figures	ii
List of Tables	ii
Executive Summary	1
Introduction	1
Methods	2
Data Management	2
Field Procedures	2
Laboratory Procedures	3
Gravimetric Analyses	3
Total Pb by ICP-MS	4
Total Zn by Flame Atomic Absorption	4
Pu Isotopes by ICP-MS	4
Pb Isotopes by ICP-MS	4
Results	5
Physical Data	5
Chronologies and Sediment Core Integrity	5
Well-Defined Chronologies	6
Undefined Chronologies	7
Flux Calculations	8
Zinc	9
Total Lead	10
Lead Stable Isotopes	10
Total Mercury	11
Discussion	12
Conclusion and Recommendations	15
References	17
Figures	F1
Tables	T1
Appendix A. Quality Assurance Project Plan	A1
Appendix B. Analytical Data Listings and Field Data	B1

List of Figures

No.	Caption	Page
1.	Location map of study lakes.	F 1
2.	Analytical data summaries for lake sediment.	F 2
3.	Plutonium activity for all sediment cores.	F 8
4.	Lockett Meadow, Arizona soil depth profile.	F 13
5.	Mercury and lead flux and concentration in post-1963 sediments.	F 14
6.	Pb stable isotope ratios for coal and gasoline potential end members.	F 16
7.	Pb isotope ratio 206/207 for potential end members and lake sediments.	F 18
8.	Metals concentrations in lake sediment versus loss-on-ignition	F 19

List of Tables

No.	Caption	Page
1.	Reservoir summary.	T 1
2.	Age models and estimated average sedimentation rates	T 1
3.	Comparison of flux and parameters used to calculate flux for 1960-1965 and 1999-2004.	T 2
4.	Average concentrations of Hg, Pb, and Zn in lake sediments	T 3
5.	Pb stable isotope analysis of potential end members.	T 4
6.	Comparison of surface sediment Hg collected and analyzed by ADEQ versus NAU.	T 5

Executive Summary

To understand the sources of mercury (Hg) to Upper Lake Mary, we collected sediment cores from Upper Lake Mary and 11 other reservoirs in northern- and central-Arizona. We performed physical and geochemical analyses on these cores to determine the chronology of sediment deposition, the concentrations of total Hg, lead (Pb), and zinc (Zn), and the stable isotope ratios of Pb. Results indicated that Upper Lake Mary and most of the other study lakes experienced non-point increases in Hg and Pb over their history. We could detect no evidence of point sources of either metals. Although we observed changes in Zn over some of the reservoir histories, we did not detect any significant Zn loading. Stable isotope data point to coal and gasoline combustion as likely sources of Pb in lake sediments. The non-point sources of Hg could be concentration of geologic Hg from within the watershed or atmospheric deposition. The growing consensus among the scientific community is that practically all watershed Hg has atmospheric deposition as the ultimate source. Because of the high affinity Hg has for organic matter, understanding the patterns of storage and release of organically-bound Hg from watersheds may be of far greater importance in managing lakes than detecting the ultimate source. Further study should be directed toward better understanding the delivery of Hg from watersheds and the biological availability of these Hg forms.

Introduction

Mercury contamination has emerged as a serious public health concern in Arizona. The Arizona Game and Fish Department in cooperation with the Arizona Department of Environmental Quality (ADEQ) and the Arizona Department of Health Services, have currently posted fish consumption advisories for eleven reservoirs statewide. Five are in northern Arizona. The origin of mercury in these reservoirs is unclear; potential sources include atmospheric deposition, geologic formations in the watershed that contain mercury, and historic land use practices.

The objective of this study is to collect and analyze sediment cores from northern Arizona reservoirs to search for temporal and spatial patterns of metals deposition.

Methods

Field and laboratory methods are outlined in this section. Complete details of standard operating procedures, quality assurance and quality control procedures, and quality assurance data are provided in the Quality Assurance Project Plan in Appendix A.

Data Management

The three data streams for the procedures below were field notes, laboratory notes, and instrumental records and calculations. All original paper files and source computer files were archived either as paper copies or in computer directories. All processed data was summarized as an Excel database. All data were verified by the principal investigator.

Field Procedures

Surface sediment cores extending from the surface/water interface to a sediment depth of about 90 cm were collected and sampled from eleven northern Arizona lakes and reservoirs. Coring locations were chosen to retrieve the thickest, undisturbed, sequential sediment package from each site. Sampling locations and summary characteristics of study lakes are provided in Table 1, Figure 1, and field data listings in Appendix B. Tables and figures for are included after the main body of the text of this document.

At each site, the principal investigator trained any new members of the field crew. A floating platform was assembled, rowed to the coring location and stabilized using ropes connected to the shore or anchor bags. A GPS receiver was used to determine and record the latitude and longitude of each sampling location. Water depth (m) was measured from the water surface to the sediment/water interface using a weighted meter tape. Notes were recorded in a field notebook.

A piston-corer (surface corer) attached to a series of steel or titanium rods was used to collect a sediment core extending from several centimeters above the sediment/water interface to about 90 cm below the interface. At Lyman and Alamo we also collected deeper cores in 1-meter intervals using a Livingstone square-rod corer, a piston corer which permits recovery of intact cores from thick sediment deposits. Each surface core was sampled using clean-hands, dirty-hands procedures and preserved in the field within four hours of collection. Each surface core was extruded from the bottom upward in 1.0 cm intervals. At each interval half the sediment

was collected into a Nalgene FLPE container and the remaining half was collected into a Whirl-pak bag. Livingstone cores were double-wrapped in plastic wrap and refrigerated until sampled in the laboratory. Notes regarding sediment descriptions were recorded in the field notebook. Nalgene containers for mercury analysis were preserved in coolers with an ice / dry ice mixture and frozen on arrival at the lab. Whirl-pak bags were preserved in the field in coolers with ice at 4°C and were placed in a refrigerator at 4° C on arrival at the lab.

After each trip, the field crew transported the coolers containing mercury samples directly back to freezers located in NAU Bilby Research Center. The field crew delivered samples for the remaining analyses to a walk-in refrigerator located in the NAU Chemistry Building. All original Field Chain of Custody forms remained with the samples until the samples were processed.

Laboratory Procedures

The samples stored in Whirl-pak bags at 4°C in the NAU Chemistry Building were sub-sampled for bulk density, moisture content, loss-on-ignition, total Pb, total Zn, Pu isotopes and Pb isotopes. Each time a sample was handled or a sub-sample created, a Laboratory Chain of Custody form was initiated. One copy of the form accompanied the sub-samples, another copy was kept with the original samples, and a third copy was kept in a laboratory logbook in Room 404 of the Chemistry Building. Analytical laboratory training was conducted by the principal investigator who reviewed standard operating procedures, demonstrated laboratory techniques, and supervised analytical staff as they practiced the procedures.

Gravimetric Analyses

Samples for gravimetric analysis were sub-sampled from the Whirl-pak bags preserved at 4°C. Samples were analyzed within 28 days of collection in the field according to the standard operating procedures provided in the project QAPP (Appendix A). Analytical procedures are based on ASTM Method D4531-86 for bulk density and APHA Method 2540G for moisture content and loss-on-ignition. Data are reported for moisture content as mass fraction moisture, for bulk density as g dry sediment / cm³, and for loss-on-ignition as mass fraction dry weight.

Total Pb by ICP-MS

Samples for total lead were analyzed using total-digestion acid extracts prepared according to the standard operating procedure provided in the QAPP (Appendix A). Samples were analyzed in the Chemistry Department at NAU following procedures based on EPA Method SW-846 6020. Data are reported as ug Total Pb / g dry sediment.

Total Zn by Flame Atomic Absorption

Samples for total zinc were analyzed using total-digestion acid extracts prepared according to the standard operating procedure provided in the QAPP (Appendix A). Samples were analyzed in the Chemistry Department at NAU following procedures based on EPA Method SW-846-7951. Data are reported as

Pu Isotopes by ICP-MS

Samples were analyzed for the mass 239, 240, and 242 isotopes of plutonium using a potassium pyrosulfate fusion procedure. Plutonium was separated from other constituents and concentrated onto an element-specific resin (TEVA), then released through an ammonium oxalate elution. The QAPP (Appendix A) provides complete documentation of preparation, analysis, and quality assurance procedures. Samples were prepared and analyzed in the Chemistry Department at NAU.

Pb isotopes by ICP-MS

Samples were analyzed for the mass 204, 206, 207, and 208 isotopes of lead using a nitric-acid extraction of dry-ashed sediment. Lead was separated from other constituents in the extract and concentrated using lead-specific resin and eluted from the resin using ammonium oxalate. The QAPP (Appendix A) provides complete documentation of preparation, analysis, and quality assurance procedures. Samples were prepared in the Chemistry Department at NAU and analyzed by NAU project personnel at the Harry Reid Center for Environmental Studies at the University of Nevada, Las Vegas.

Results

Physical Data

We analyzed samples from each core at 1-cm intervals for three physical parameters: moisture content, bulk density, and loss-on-ignition (LOI). Moisture content and bulk density tended to be inversely related and both are measures of compression in the sediment column. Moisture content is the mass or weight fraction of water in the sediment (mass of water divided by total mass of sample). Bulk density is the dry mass of sediment occupied by a fixed volume of in-situ sediment, expressed as grams dry sediment per cubic centimeter. For example, low bulk density reflects a combination of low soil density (e.g., organic matter is less dense than sand) and high porosity.

LOI is a measure of the organic content of the sediment expressed as the loss in mass on ignition at 550°C divided by the original dry mass of the sample. Organic matter in the sediment can be derived from within the lake by primary productivity or can be terrestrial organic matter washed into the lake with runoff. LOI varies based on the absolute input of organic carbon and the dilution of that carbon relative to the total mass of sediment by inorganic sediment washed into the lake. We observed, for example, bands of dark sediment in the Lyman and Alamo cores which we believe reflect summer periods of high biological productivity and little input of inorganic sediment from the watershed. These dark bands were separated by light-colored zones of coarser inorganic sediment from storm runoff.

The Upper Lake Mary and Lyman cores showed the greatest systematic variability in physical parameters. In Upper Lake Mary, two distinct peaks in LOI appear at 27 and 39 cm and are associated with increases in moisture content and decreases in bulk density (Figure 2a).

In Kinnickinick, Long, Carnero, Nelson, and Ashurst, bulk density increased toward the base of the core, presumably due to compression. The weight of overlying sediment collapses pore spaces occupied by water. The increase in bulk density with depth was particularly abrupt in Kinnickinick, Long, Carnero, and Nelson, which may be associated with the onset of permanent flooding after impoundment.

Chronologies and Sediment Core Integrity

We attempted to establish chronologies to relate positions in each sediment core to known dates. Well-defined chronologies allow us to compare changes across lakes. In this study we

used two age markers: radio-isotopic analysis and date of impoundment. Radiometric dating provides a marker for the peak of above-ground atomic testing in 1963 (Beck and Bennett, 2002). The characteristic change in radioactive fallout over the period of 1954 to about the 1970s also provides an indication of sediment disturbance and remixing. A plot of $^{239+240}\text{Pu}$ versus depth in the core, for example, which has a single, well-defined peak indicates that sediments have been deposited sequentially over time with a minimum of disturbance. Broad or multiple peaks indicate disturbance and complicate interpretation of data from the core.

We also attempted to relate the date of impoundment of each lake with observations of transitions in physical characteristics of the cores that indicate the onset of permanently-flooded conditions. Reservoirs in this study had several possible origins. Some reservoirs were existing playa-like lakes or wetlands which had dams constructed to create recreational features (e.g., Ashurst Lake), or to improve the reliability of water supply for cattle grazing (e.g., Soldiers and Long Lakes). Others were riverine systems without standing water (e.g., Willow Springs, Nelson, Lyman, and Alamo). Lakes such as Upper Lake Mary and Carnero have more complicated histories, which made the use of the date of impoundment problematic.

The quality of the chronologies for each lake determined which lakes were used for analysis of flux and was the basis in three cases (Willow Springs, Lower Lake Mary, and Stoneman) for excluding lakes from comparative analysis for several analytical parameters.

Well Defined Chronologies

Figures 3a through 3e show the data for $^{239+240}\text{Pu}$ versus core depth for the study lakes. Upper Lake Mary, Ashurst, Lyman and Carnero showed quite well-defined peaks in plutonium activity and we assigned positions for the 1963 marker with confidence. On the basis of this marker, we estimated sedimentation rates for the period 1963 to present (Table 2).

Upper Lake Mary showed a very well defined 1963 peak at 13cm, with little Pu activity below or above the base of the peak. The lake was impounded in 1941 and according to the Arizona Game and Fish Department (Benedict, personal communication, 2005) was a riverine wetland prior to impoundment. We observed a massive peat layer at 39cm (Figure 2a) and assigned the year 1941 to this location.

Ashurst Lake showed a broad single peak with maximum Pu activity at 14cm. Although the lake was impounded in 1954, we did not assign that year to the base of the core, because the lake

was an existing, but likely intermittent, water feature. We extrapolated the 1963-present sedimentation rate below 14 cm.

At Lyman Lake we collected an 80-cm surface core and a series of 1-meter Livingstone cores starting at about 20 cm below the sediment-water interface. Pu dating of both cores provided the basis for an excellent match between the surface and Livingstone cores. Lyman had a well-defined 1963 peak at 98cm, but also showed minor peaks at about 170 and 250 cm, indicating some remixing in that interval. We assigned the base of the core at 475 cm the impoundment date of 1910. The reservoir was clearly riverine prior to impoundment and the base of the core was clearly the transition between aquatic and terrestrial sediment.

Carnero Lake showed a single, well-defined peak at 17.5 cm; however a troubling anomaly with Carnero Lake is that the date of impoundment, according to Arizona Game and Fish Department records (Dreyer, personal communication, 2005), was 1979. According to Dreyer (2005), prior to impoundment the area did not maintain a permanent pool. The USGS topographic quadrangle (Greens Peak, Arizona), which was drawn from photographs taken in 1967, shows the lake in its present configuration, with no indication that it was added in the only other revision to the map in 1969. We are searching for aerial imagery of the site taken in the period from the 1940s to the 1960s to resolve the origin of the sediment. Because the curve is so well defined, however, we included Carnero in further comparative analysis.

As with Lyman, Kinnickinick Lake showed a distinct peak at a high position in the core (7 cm), but minor peaks at lower positions. According to the peak, Kinnickinick also showed the lowest sedimentation rate (0.17 cm/yr, Table 2).

Alamo Lake was impounded in 1968, well after the peak in plutonium activity. The lake was riverine prior to impoundment and the base of our core showed clear signs of terrestrial sediment at 440 cm. We thus based our estimate of the average sedimentation rate of 12.2 cm/year (Table 2) on this single marker.

Undefined Chronologies

We were unable to establish reliable chronologies for Nelson, Willow Springs, Lower Lake Mary, and Stoneman for reasons specific to each lake. Data from these cores did, however, yield valuable information.

Impounded in 1892 (Dreyer, 2005) Nelson Reservoir was the oldest reservoir in this study. Coring revealed the lake has sediment column of about 70 cm. At 57 cm we observed an abrupt transition from dark, un-differentiated, organic sediment (gyttja) above, to lighter, low-organic clay below (appendix, field notes). This position corresponded to an increase in bulk density and a decrease in moisture content with depth (Figure 2e). Ordinarily we would have assigned the date of impoundment to this clear transition; however Pu analysis showed a very narrow, high-magnitude peak at 55 cm (Figure 3e). The 239 and 240 isotopes of plutonium did not exist prior to the atomic era, so the source for this Pu must be in the 1950s or later. The shape of the Pu curve suggests there was zero sediment accumulation until the 1950s, low sedimentation until the mid-1960s, and extremely high sedimentation from the 1960s to present. We are unable to explain sedimentation in this lake and exclude Nelson from chronometric analysis.

Although Willow Springs was a riverine system prior to impoundment in 1967, we were able to collect a 38-cm sediment core. Unlike other reservoir cores in this study, which were typically fine-grained, the core from Willow Springs had a high fraction of sand and low fraction of silt and clay. Pu dating (Figure 3e) revealed low Pu increasing to a maximum at the core top. This shape is highly characteristic of terrestrial soils. A soil profile from Lockett Meadow showing this trend is presented in Figure 4. (Ketterer et al., 2003). We concluded that the core consisted primarily of pre-impoundment terrestrial soil and excluded Willow Springs from comparison with other aquatic sediment cores. We did however, consider concentrations of analytes in the core to reflect terrestrial soil conditions.

Lower Lake Mary and Stoneman Lake both showed Pu curves with relatively high Pu activities and indistinct peaks (Figure 3e). These are characteristic of periodic desiccation and remixing. As a result we did not attempt to construct chronologies of these lakes.

Flux Calculations

Bulk density measurements collected with the physical data, and sedimentation rates estimated from the chronometric analysis enabled us to estimate the flux, or annual delivery, of sediment and elements to each lake for which we have reliable chronologies. The form of the flux calculation for an element is

$$\begin{aligned} \text{Flux} &= \text{Metal Concentration} \times \text{Bulk Density} \times \text{Sedimentation} \\ [\text{g/cm}^2/\text{yr}] &= [\text{g metal} / \text{g dry sediment}] \times [\text{g dry sediment} / \text{cm}^3] \times [\text{cm/yr}] \end{aligned}$$

Flux calculations can enable certain types of pollutant loading to be detected. For example, a constant areal (say g/m^2) delivery of an atmospheric pollutant may be observed to fluctuate in a sediment record due to changes in sedimentation patterns. Increased sedimentation rates would dilute the concentration and decreased sedimentation would concentrate the pollutant.

Flux calculations normalize for changes in sediment delivery; however, there is a problem in applying flux calculations associated with estimates of both bulk density and sedimentation. Bulk density tends to increase lower in the core due to compression. This results in a higher effective sedimentation rate toward the bottom of the core (e.g., a sediment layer 1.00-cm thick in 1945 may have been compressed to 0.75 cm by overlying sediment in subsequent decades). High-resolution dating, such as counting annual layers in sediment, can correct for this effect. Our age models, however, are only capable of estimating average sedimentation between known dates in the sediment record. As a result, sedimentation rates are probably overestimated toward the top of the core and underestimated toward the bottom.

Because of errors inherent in the flux calculation, we only calculated flux for lakes which have well-characterized age models. We calculated flux for the time period between 1963 and present for these lakes. This period represents our best estimates for sedimentation rates and corresponds to upper portions of sediment cores, which are likely less affected by compression.

Flux calculations are summarized in Figure 5a for Hg and Figure 5b for Pb and in Table 3. Elemental concentrations are included in Figures 5a and 5b for comparison with fluxes. The influence of relative magnitudes of sedimentation and bulk density can be seen by comparing flux with concentration for Carnero and Lyman. Carnero had high concentrations of both Hg and Pb relative to Lyman. The low bulk density of sediments in Carnero and the high sedimentation rates in Lyman resulted in low flux of both Hg and Pb for Carnero relative to Lyman. Similarly high sedimentation in Soldiers and low sedimentation in Kinnickinick place them at extremes for elemental flux.

Zinc

Although present in geologic materials in watershed, changes in sediment Zn are generally associated with atmospheric deposition of high-temperature combustion products (Kim et al., 2000) and from runoff associated with tire wear and other automobile emissions (e.g., Gualtieri et al., 2005; Blok 2005). About half of the lakes in this study showed a clear increase in Zn from

the base of the core Figures 2a through 2e. All lakes except for Willow Springs had an average Zn of 153 ug/g (Table 4). Willow Springs had considerably lower sediment Zn at 70 ug/g, but as was discussed earlier, this may reflect terrestrial soil rather than aquatic sediment. Upper Lake Mary had the highest single concentration of Zn of 1,585 ug/g at 38 cm. This corresponds to a peat layer at the presumed time of impoundment. The highest concentrations of Pb occur in this part of the core, but not the highest concentrations of Hg (Figure 2a).

Regardless of changes in concentration lower in the cores, Upper Lake Mary, Ashurst, and Kinnickinck show a clear trend of increasing Zn concentration in the top 4 or 5 cm of the cores (Figure 2). These lakes are all located in the same general region, on or at the margin of the Anderson Mesa. The other two nearby lakes, Long and Soldiers, do not show this trend. Of all the lakes, only Upper Lake Mary and Lower Lake Mary are subject to direct highway runoff, although no clear effect of this runoff is evident.

Total Lead

Total lead showed clear increases from the base of the core in Upper Lake Mary, Ashurst, Kinnickinck, and Carnero. The remaining lakes all showed at least some excursions of higher values than at the base. Pb concentrations at the base of cores averaged 23 ug/g, while averages across entire cores ranged from 20 ug/g in Long to 54 ug/g in Lower Lake Mary.

Analysis of Pb flux (Figure 5 and Table 3) indicates that Soldiers, Lyman, and Alamo received the greatest quantity of Pb. These high delivery rates are associated with high sedimentation rates, and in the case of Soldiers high bulk density, rather than unusually high Pb concentrations.

Lead Stable Isotopes

Of the four stable isotopes of lead (mass 204, 206, 207, and 208), all but the mass-204 isotope are radiogenic. These isotopes are the decay products of other radioactive isotopes. As a result, the ratios of these isotopes relative to the mass-204 isotope vary depending on the age of the parent geologic formation and the quantities of parent radioisotopes (Faure, 2005). This phenomenon has been useful in fingerprinting sources of Pb in environmental contamination studies (e.g., Graney and Erikson 2004; Hurst 2002; Renberg et al., 2002).

Potential sources of Pb which have distinctive isotope ratios are termed *end members*, as they form the extreme bounds of plots of the isotope data. We considered two principal sources for Pb: gasoline from the leaded-gasoline era and coal. The isotopic signature for lead from gasoline is now well understood and is known to vary over the production life of leaded gasoline from 1924 to mid-1960s. We use the ALAS (recite acronym) model to define the end-member 206/207 Pb ratio for gasoline over time (Hurst 2002).

The other likely end member for Pb isotopes is coal. We analyzed coal from four northern-Arizona / northwest-New Mexico mines which provide coal to nearby power plants. The data are summarized in Table 5 and plotted as combinations of isotope ratios in Figure 6. Figure 6a plots the likely end members, along with 1-standard-deviation error bars for the samples analyzed. The gasoline data were taken from literature values for California gasoline from the mid-1960s (Chow and Johnstone, 1965). We also included data from Willow Springs, which likely represents terrestrial soil conditions. These data indicate that Pb isotope values are constrained by gasoline, at the highest end of values for isotope ratios, to coal from the Black Mesa mine, at the lowest end of values.

Figure 6b re-plots these data in addition to observations from the lake sediment samples. All but the Alamo and Stoneman samples fall generally between the end-member values. Lyman sediments also deviate somewhat from end-member combinations on plots of 208/206 versus 204/206 and 208/206 versus 207/206.

Figure 7 shows the average 206/207 ratio of coal plotted as a constant value versus date, along with the gasoline signature for 206/207 from the ALAS model (Hurst 2002) and lake sediment data. These data show that 206/207 varies in Upper Lake Mary and Ashurst between the end members for gasoline and coal until the mid-1970s, then stabilizes from the 1970s to present. Observations from other lakes plot close to the average value for coal, except for Alamo, which has much higher values for 206/207. It is possible that other lakes demonstrate distinct trends in 206/207 over time, but we only have a limited number of observations for lakes other than Upper Lake Mary and Ashurst (Figure 2).

Total Mercury

All lakes except Alamo showed clear increases in Hg from the base of the core (Figure 2 and Table 4), although the patterns of change over the length of the cores varied from lake to lake.

Hg at the base of cores averaged 36 ng/g and at the tops of cores the average Hg was 80 ng/g. Only Nelson had a core-wide average Hg (33 ng/g) less than the average Hg of core base values. Hg in Alamo showed systematic changes (changes that occurred over several data points), but did not vary more than 15 ng/g from the mean of 65 ng/g over the length of the core.

Hg flux is plotted in Figure 5. As with Pb flux, Hg flux is strongly influenced by bulk density and estimates of sedimentation. As a result, Soldiers and Lyman demonstrate the highest fluxes of about 30 ngHg/cm²/yr, while other lakes show progressively lower fluxes. The high sedimentation rates for Alamo result in Hg delivery more than an order of magnitude higher than the other lakes.

We compared surface sediment Hg concentrations from ADEQ sampling and our study in Table 6. NAU values for Upper Lake Mary were significantly higher than ADEQ values, however ADEQ data show much higher variability. The small number of samples for other sites does not permit statistical comparison, but NAU values were within 10 ng/g Hg for the other three sites. Two likely causes for the differences in the data are spatial heterogeneity in sediment Hg and inter-laboratory differences. ADEQ sampling techniques use a bulk sampling device that samples the top 5 to 10 cm of sediment, vertically integrating the sample. In lakes such as Willow Springs, Hg changes rapidly with depth. Variations in vertical integration would affect the average value. Hg may well be spatially variable across the surface of the lake. The high variability among ADEQ samples for Upper Lake Mary may be related to this spatial variability. Additional analysis of spatial heterogeneity and inter-laboratory analyses of reference sediment samples would address causes for differences between ADEQ and NAU samples.

Discussion

Total Hg, Total Pb, Pb Isotopes, and Zn all showed changes in sediment concentration, which in some way must be anthropogenic. Possible sources of metals in the sediments of these reservoirs include point sources from discrete releases of the metals, crustal sources that may be detected as changes in concentrations over time due to watershed disturbances, or atmospheric sources. There were no indications of point sources for Hg, Pb, or Zn; any patterns of change detected in one lake were also detected in other lakes, usually in the same geographic area. An exception was the high concentrations of Pb and Zn at the 39-cm position in the Upper Lake

Mary core (Figure 2). This excursion, however was clearly related to organic trapping of metals in peat during the likely pre-impoundment period in the lake.

In principle, it is possible that a significant source of metals is a crustal source that is concentrated by organic matter. Metal ions have a high affinity for organic carbon (Stumm and Morgan 1996), so the organic carbon pools in the terrestrial or aquatic ecosystems may have acted as a sink for metals, as suggested by the high concentrations of Zn and Pb toward the base of the Upper Lake Mary core. Plots of Zn, Hg, and Pb versus LOI, a measure of organic carbon, indicate generally positive correlations between metals and organic carbon on a lake-specific basis (Figure 9). These correlations do not reveal the origins of the metals, but do provide a mechanism to explain how it may be possible for crustal or anthropogenic metals to accumulate in concentrations higher than their original mineral concentration. From a kinetic standpoint, the amount of crustal Hg available for organic uptake is limited by the rate of weathering. It is beyond the scope of this study to assess the relative theoretical contribution of Hg from atmospheric loading sources versus crustal sources through weathering, but the exercise would be straightforward.

Concentration of crustal metals by organic carbon may explain some of the variability in metals, but there are clear indications of anthropogenic sources in the patterns of Pb stable isotope change and in the similarity of changes in metals concentrations over time across watersheds. The Pb isotope record clearly shows variation in Upper Lake Mary and Ashurst between the two end members of coal and leaded gasoline (Figure 6). Only Upper Lake Mary, Ashurst, and Lyman were analyzed at sufficient resolution to detect temporal trends. The trends were similar for Upper Lake Mary and Ashurst. Pb ratio plots (Figure 6b) indicate that all lakes except Alamo, Lyman, and an observation from Stoneman, fall in a straight line between the end members of gasoline and coal. This does not exclude other sources for the Pb in these sediments, but is consistent with a combination of these two. Additionally, a coal combustion source for Pb may also explain some of the sources of Hg loading, as Hg is released with coal combustion (e.g., Yudovich and Ketris, 2005).

Lyman and Alamo have distinctive Pb isotope ratios that did not necessarily plot in a straight line between the gasoline and coal end members (Figure 6b). Clearly there is a missing end member that we did not sample, of either crustal or anthropogenic origin. Alamo is geographically distant from other lakes and may well have different sources of atmospheric

deposition. In the case of Lyman, the unique ratios did not appear in samples from nearby lakes Nelson and Carnero, but we only analyzed a small number of samples from these lakes and the trend may be present but undetected. Other possible end members require investigation and include such sources as cement plants and smelters.

The Pb isotope record points to gasoline combustion as a contributing source which may be related to Zn loading, but not to Hg loading. Hg is not a significant component of gasoline-combustion emissions (Conaway, et al., 2005) so would not be expected to co-vary with Pb. Zn, however, may be linked to gasoline combustion; not through emissions, but through roadway runoff associated with automobiles (e.g., Gualtieri et al., 2005; Blok 2005). Upper Lake Mary would be the likeliest candidate for metals deposition from highway runoff, but shows no clear pattern of increased Zn. Episodes of high Zn concentration occur at about 17, 28, 34 and 39 cm in the core, but all correspond with increases in organic carbon. Each of these may correspond with dry or low-water periods in the lake history when soil or peat may have formed.

Hg concentrations show an even clearer pattern of increase with time than Pb or Zn. As with the other metals, there does not appear to be any point source of Hg. Hg flux calculations (Figure 5) separate the lakes somewhat in terms of their delivery of Hg to the sediments. Lakes with low sedimentation or high bulk density tended to have higher Hg budgets.

Sensitivity of flux to sedimentation rate also points to the importance of crustal concentrations of Pb and Hg. Alamo, for example had Hg flux more than an order of magnitude higher than any other lake. Even corrected for watershed size, the delivery of crustal Hg appears to dominate the total Hg budget of this lake due to its high sedimentation. Crustal Hg is probably far less biologically available than organically-bound Hg, but the analysis for total Hg does not distinguish between the forms. More sophisticated analysis to separate the forms would be appropriate

The focusing of crustal Hg, and metal ions in general, by organic carbon is possible, however the consensus among Hg researchers is that increases in Hg in ecosystems is caused by atmospheric deposition. In a review of Hg sequestration in forests and peatlands, Grigal (2003) states, "Nearly all Hg in vegetation is derived from the atmosphere." Our observations are consistent with a non-point source of Hg. Upper Lake Mary, Ashurst, and Kinnickinick all have unconnected watersheds, but Hg concentrations varied similarly. In addition, Carnero, which is distant from the other three, showed similar patterns in Hg.

From a lake management standpoint, the question of whether the ultimate source of Hg is atmospheric or crustal may be less relevant than how Hg is stored and released from watersheds. Because surface areas of reservoirs tend to be far smaller than their watersheds, the greatest proportion of an atmospheric Hg load must be transported through terrestrial ecosystems. Studies of Hg in watersheds concluded that the inorganic Hg^{2+} form of mercury has such a high affinity for organic carbon that it is rapidly incorporated into soil litter and living biomass (e.g., Ravichandran 2004 and Grigal 2002). Of great relevance in aquatic ecosystem studies, then, may be how Hg in watersheds is sequestered and released.

A corollary to questions regarding the storage and release of Hg in is how atmospheric-derived Hg behaves after arrival in the reservoir. In reservoirs with high sedimentation rates, such as Alamo and Lyman, most of the Hg is effectively removed from the ecosystem through burial. Most Hg arrives in the inorganic form bound to organic matter (Ravichandran 2004). If that organic carbon is labile and easily dissolved, it may be far more biologically available than Hg incorporated into massive charcoal, associated with fire events (Caldwell et al., 2000). In summary, although the ultimate source of most Hg in aquatic ecosystems may be atmospheric, the proximate processes Hg undergoes in terrestrial watersheds may be of far greater importance in lake management.

Conclusions and Recommendations

Our analysis of sediment cores from northern- and central-Arizona reservoirs detected patterns of change in Hg, Pb, and Zn delivery to aquatic sediments. Similarities in these patterns of change across watersheds point to non-point sources of the metals, either through concentration of crustal sources of the metals, or more likely through atmospheric deposition. Pb stable isotope analysis indicates a gasoline source for at least some of the Pb deposition. Pb stable isotopes detected in the sediments are also consistent with a coal source, indicating power plants as a possible source of some deposition. Gasoline combustion explains some of the Pb deposition, and perhaps some of the Zn loading, but not the Hg loading. Hg is not a significant component of gasoline combustion. Observed increases in both Hg and Pb point to a coal combustion source, which can deliver both metals through atmospheric deposition.

We observed increases in Hg over time in all lakes except Lower Lake Mary, which has a highly disturbed sediment record, and Willow Springs Reservoir, which appears to have

terrestrial rather than aquatic sediment. As with the other metals, there is no indication of point-sources of Hg in any of the study lakes. The likely non-point sources are geologic or atmospheric. Although it is possible that the ultimate source of Hg in these lakes is geologic from within the watershed, the growing consensus among the scientific community is that the ultimate source of Hg in ecosystems is atmospheric.

Whether the source is geologic or atmospheric, transformations of Hg with organic carbon in the watershed prior to delivery to the reservoir appear to control the Hg budget of lakes. From a lake management standpoint, the most important questions regarding Hg in aquatic ecosystems relate to (1) Hg storage in and release from watersheds and (2) the biological availability of the organic carbon forms associated with the Hg delivered to aquatic ecosystems.

We recommend additional study in two areas: identifying the relative contribution of geologic Hg from within the watershed and characterizing the biological availability of Hg delivered to lakes. Understanding the aquatic Hg budget is an essential early step in determining sources of Hg in the food web. We observed in Alamo Reservoir, for example that although Hg delivery is high, the supply of biologically available Hg may be relatively low due to burial. Similarly, Hg bound in woody biomass delivered to lakes associated with wildfires may be far less biologically available than Hg incorporated into dissolved organic carbon.

References

- Beck, H.L. and B.G. Bennett, 2002. Historical Overview of Atmospheric Nuclear Weapons Testing and Estimates of Fallout in the Continental United States, *Health Phys.* 82(5):591-608.
- Blok, J., 2005. Environmental exposure of road boarders to zinc. *The Science of the Total Environment*, Article in press, preprint.
- Caldwell, C.A., C.M. Canavan, and N.S. Bloom, 2000. Potential effects of forest fire and storm flow on total mercury and methylmercury in sediments of an arid-lands reservoir. *The Science of the Total Environment*, 260:125-133.
- Chow, T.J. and M.S. Johnstone, 1965. Lead isotopes in gasoline and aerosols of Los Angeles Basin, California. *Science*, 147:502-503.
- Conaway, C.H., R.P. Mason, D.J. Steding, and A.R. Flegal, 2005. Estimate of mercury emission from gasoline and diesel fuel consumption, San Fransisco Bay area, California. *Atmospheric Environment*, 39:101-105.
- Dreyer, R., 2005. Arizona Game and Fish Department, Pinetop Region I Office, Pinetop, Arizona, 928-367-4281.
- Faure, G., 2005. *Isotopes: Principles and Applications*. 3rd Edition, Wiley, Hoboken, NJ, 896 pp.
- Grigal, D.F., 2003. Mercury sequestration in forests and peatlands: A review. *J. Environ. Qual.* 32:393-405.
- Grigal, D.F., 2002. Inputs and outputs of mercury from terrestrial watersheds: A review. *Environ. Rev.*, 10:1-39.
- Hurst, R.W., 2002. Lead isotopes as age-sensitive genetic markers in hydrocarbons. 3. Leaded gasoline, 1923 – 1990 (ALAS Model). *Environmental Geosciences*, 9(2):43-50.
- Ketterer, M.E., K.M. Hafer, C.L. Link, D. Kolwaite, J. Wilson, and J.W. Mietelski, 2003. Resolving global versus local/regional Pu sources in the environment using sector ICP-MS. *J. Anal. At. Spectrom.*, 19:241-245.
- Graney, J.R. and T.M. Erikson, 2004. Metals in pond sediments as archives of anthropogenic activities: a study in response to health concerns. *Applied Geochemistry*, 19:1177-1188.
- Gualtieri, M., M. Andrioletti, C. Vismara, M. Milani, M., Camatini, 2005. Toxicity of tire debris leachates. *Environment International*, Article in press, preprint.
- Kim, G., J.R. Scudlark, and T.M. Church, 2000. Atmospheric wet deposition of trace elements to Chesapeake and Delaware Bays. *Atmospheric Environment*, 34:3437-3444.
- Ravichandran, M., 2004. Interactions between mercury and dissolved organic

matter—a review. *Chemosphere*, 55:319-331.

Renberg, I., M.L. Brannvall, R. Bindler, and O. Emteryd, 2002. Stable lead isotopes and lake sediments – a useful combination for the study of atmospheric lead pollution history. *The Science of the Total Environment*, 292:45-54.

Stumm, W. and J.J. Morgan, 1996. *Aquatic Chemistry*. 3rd Edition, Wiley Interscience, New York, 220 pp.

Yudovich, Y.E., and M.P. Ketris, 2005. Mercury in coal: a review Part 2. Coal use and environmental problems. *International Journal of Coal Geology*, Article in press, preprint.

FIGURES

Figure 1. Site Location Map.

To Be Added.

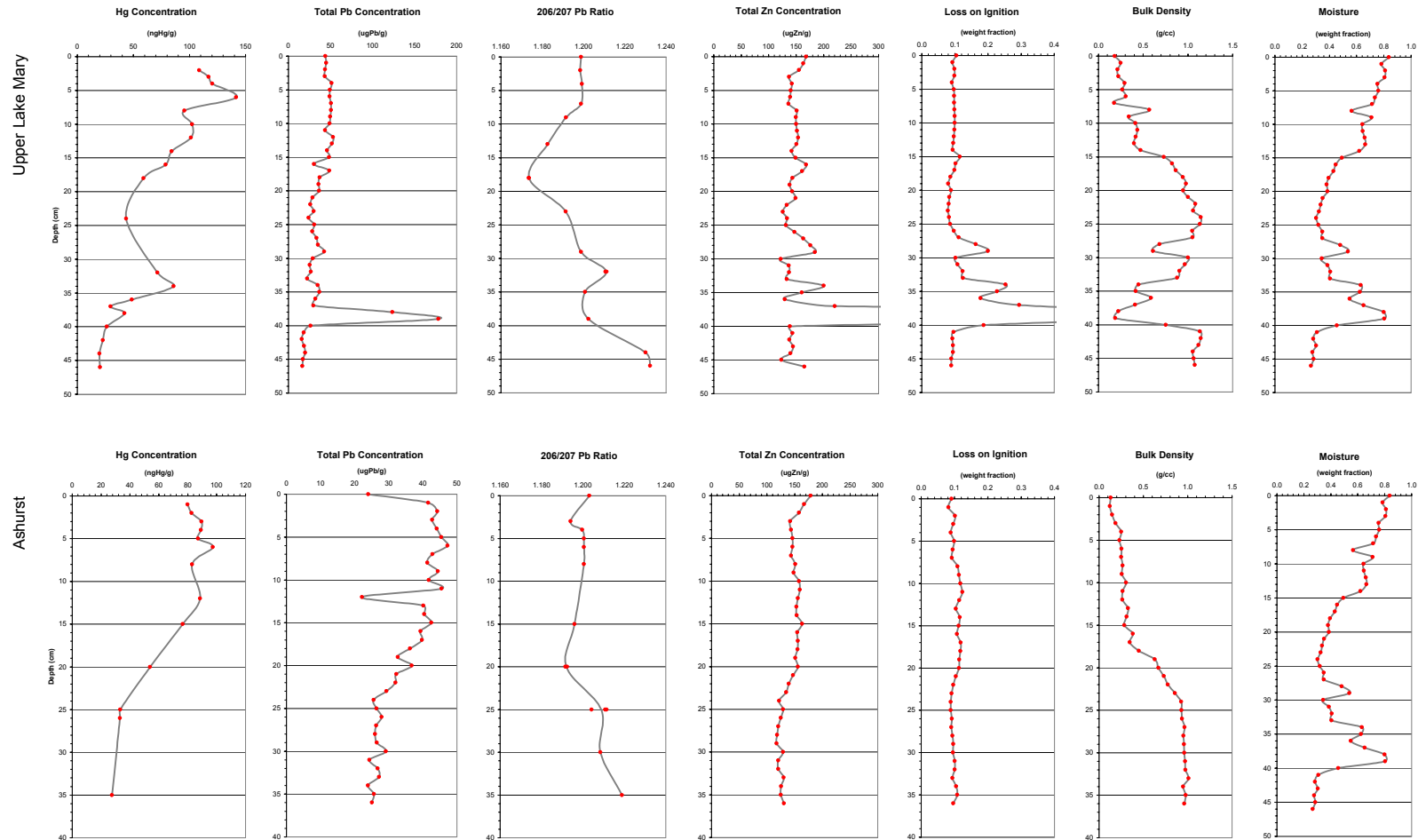


Figure 2a. Data summary for Upper Lake Mary and Ashurst Lake.

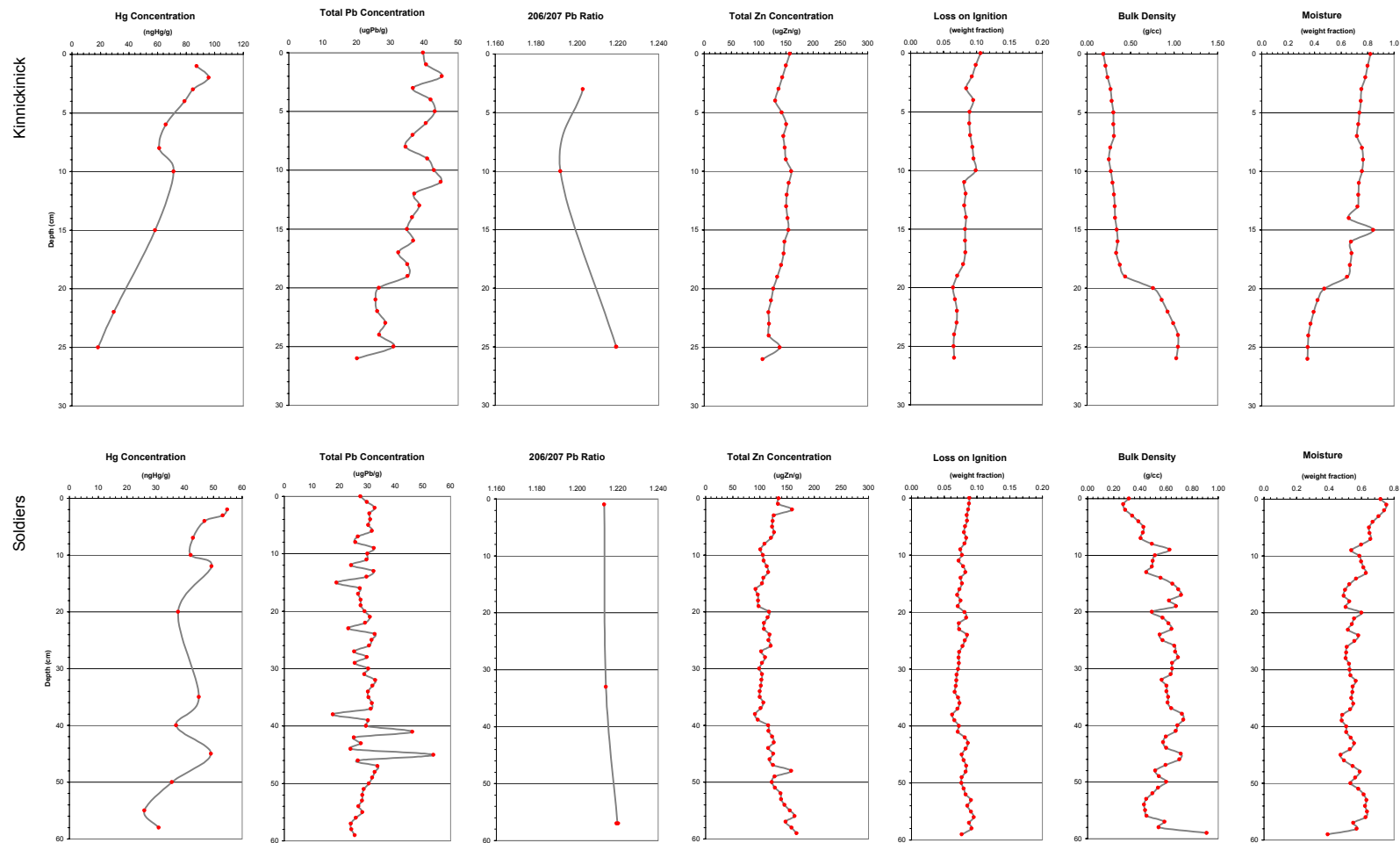


Figure 2b. Data summary for Kinnickinick and Soldiers Lakes.

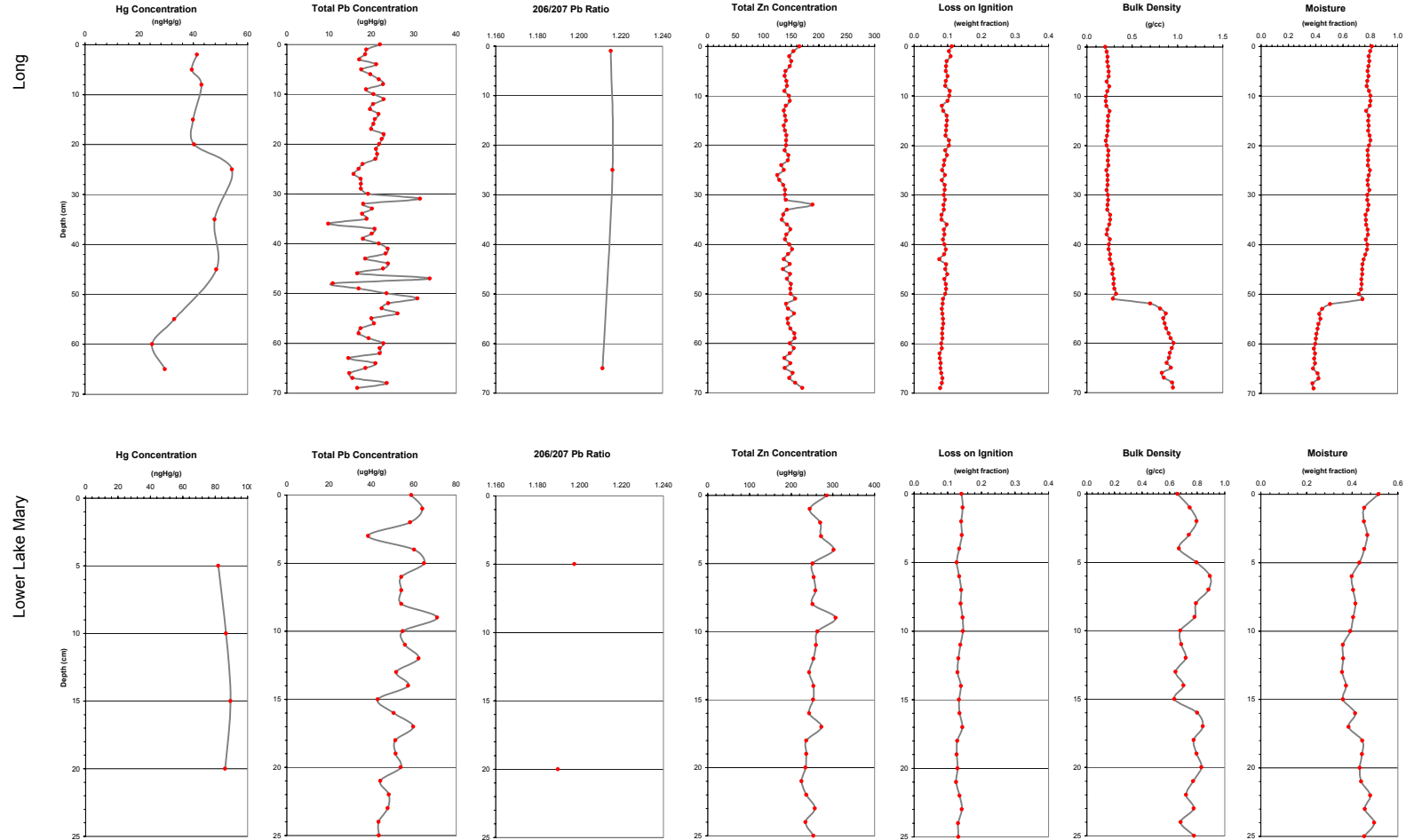


Figure 2c. Data summary for Upper Lake Mary and Ashurst Lake.

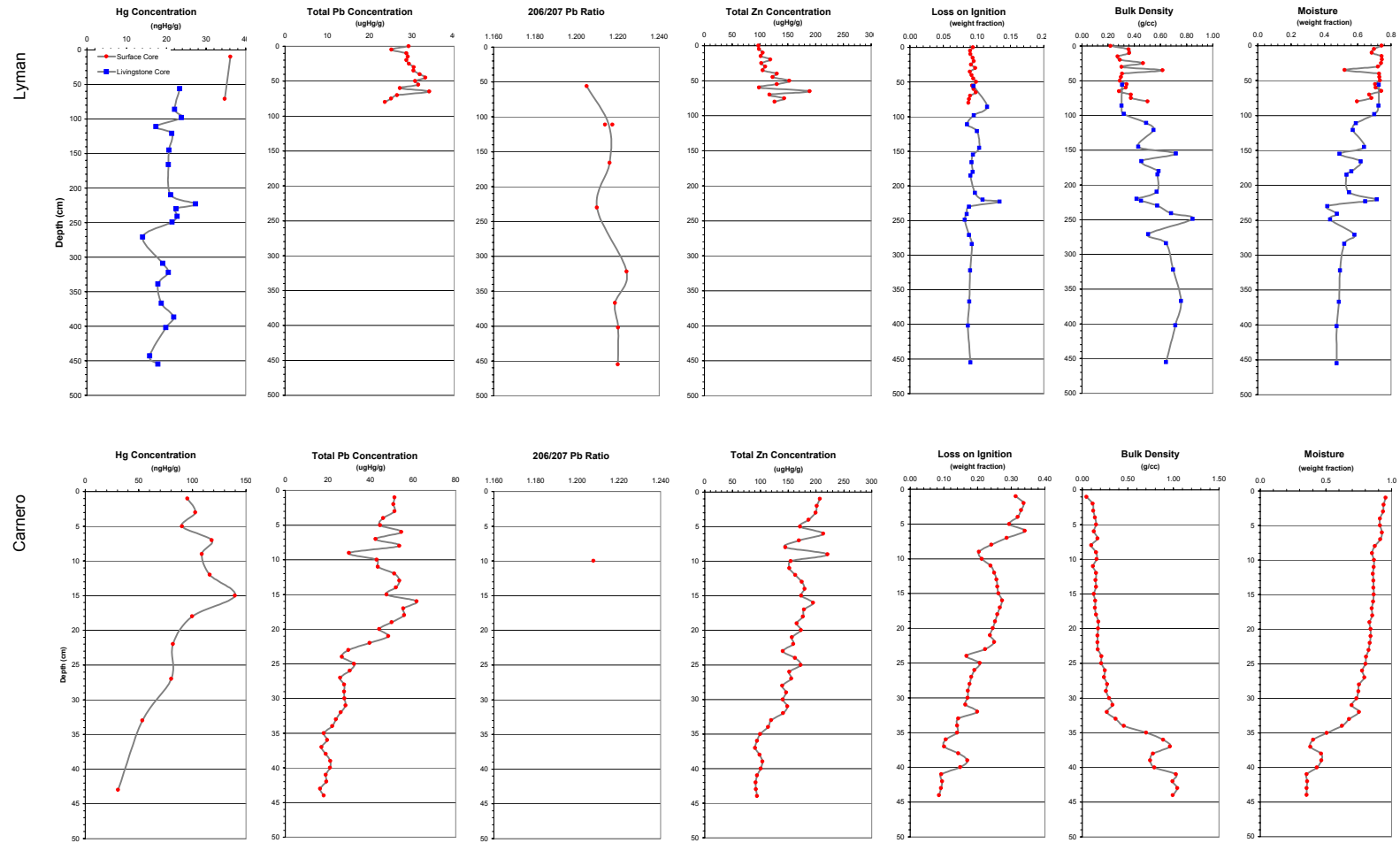


Figure 2d. Data summary for Lyman and Camero Lakes.

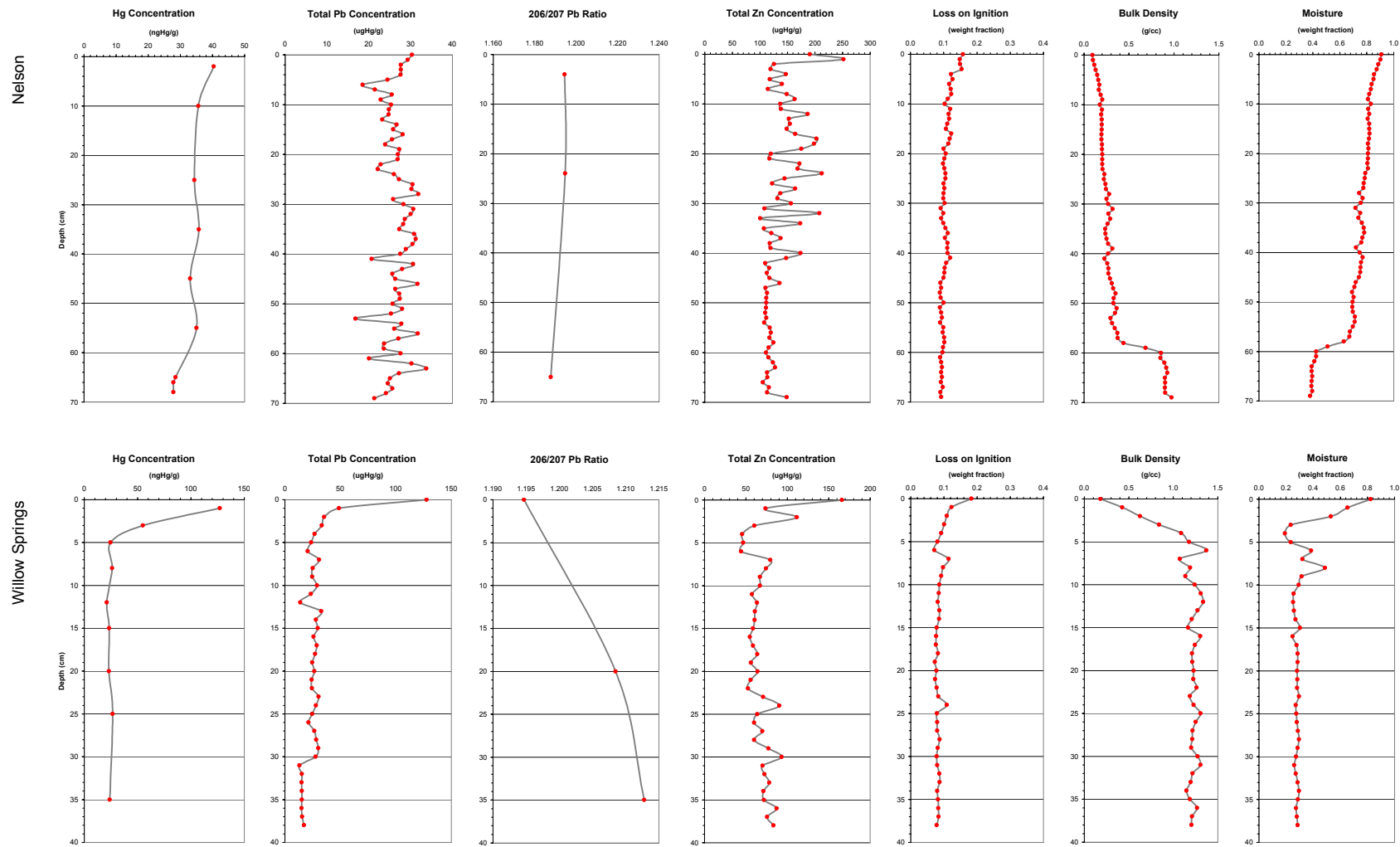


Figure 2e. Data summary for Nelson and Willow Springs Lakes.

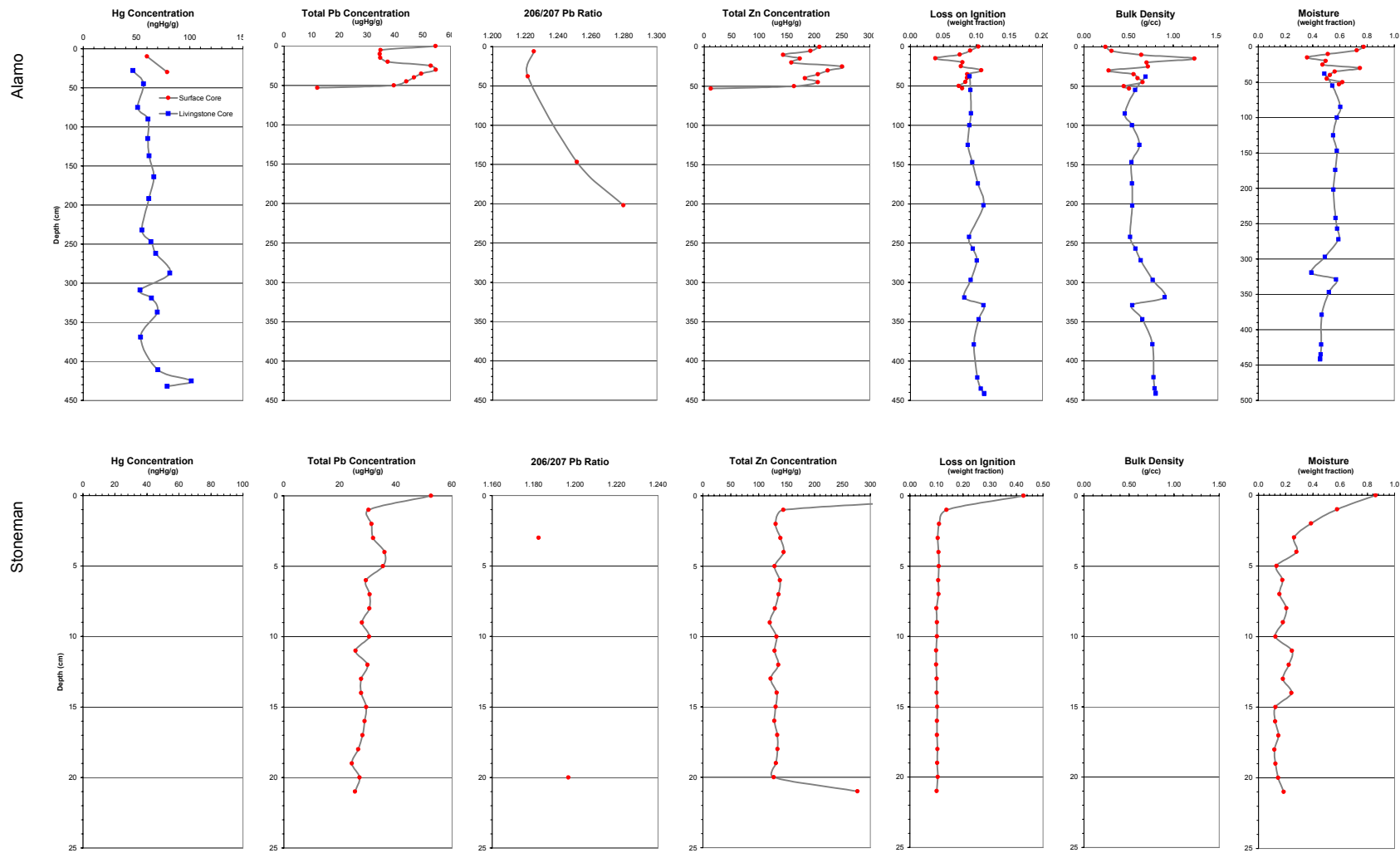


Figure 2f. Data summary for Alamo and Stoneman Lakes.

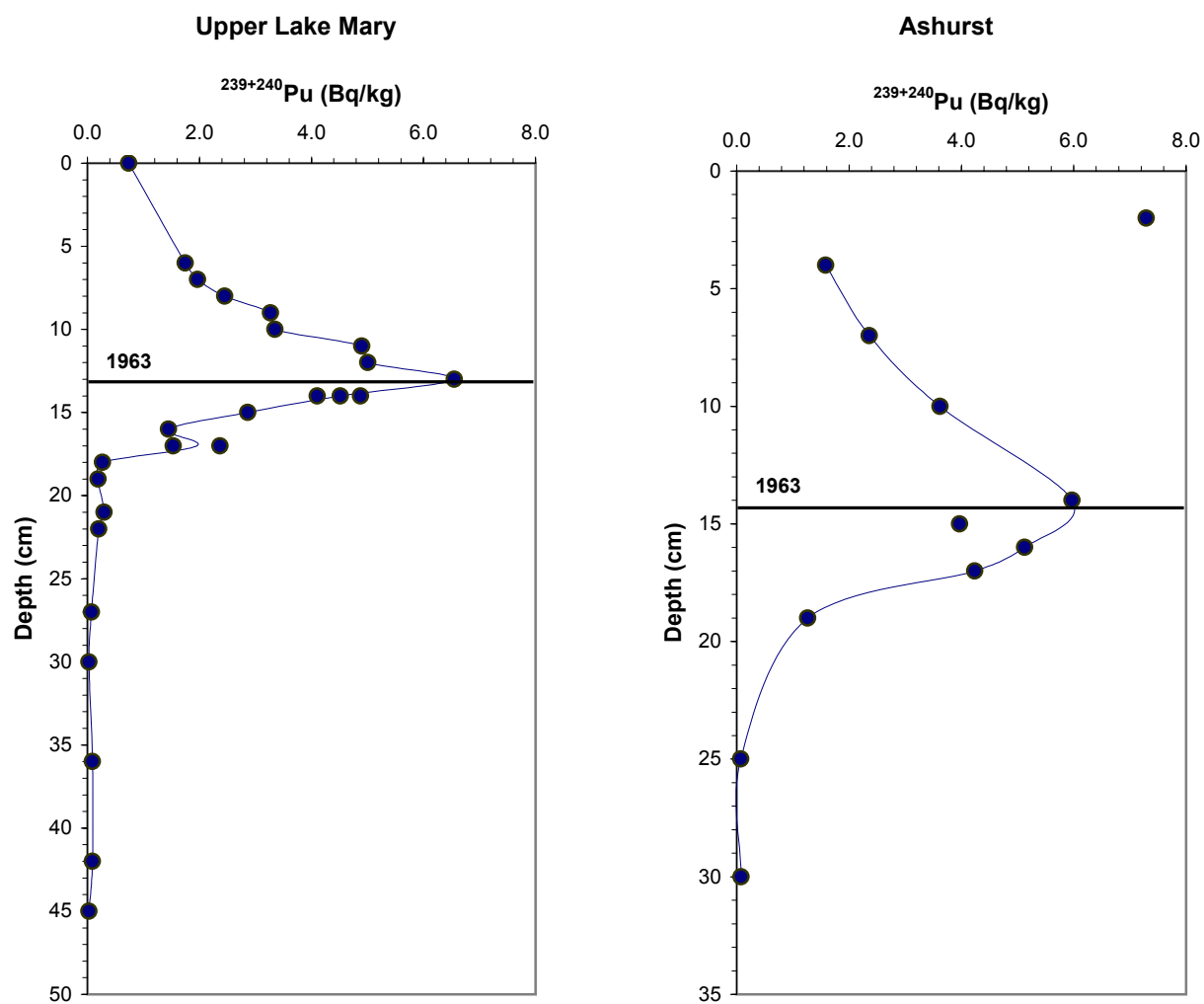


Figure 3a. Plutonium activity for Upper Lake Mary and Ashurst Lake.

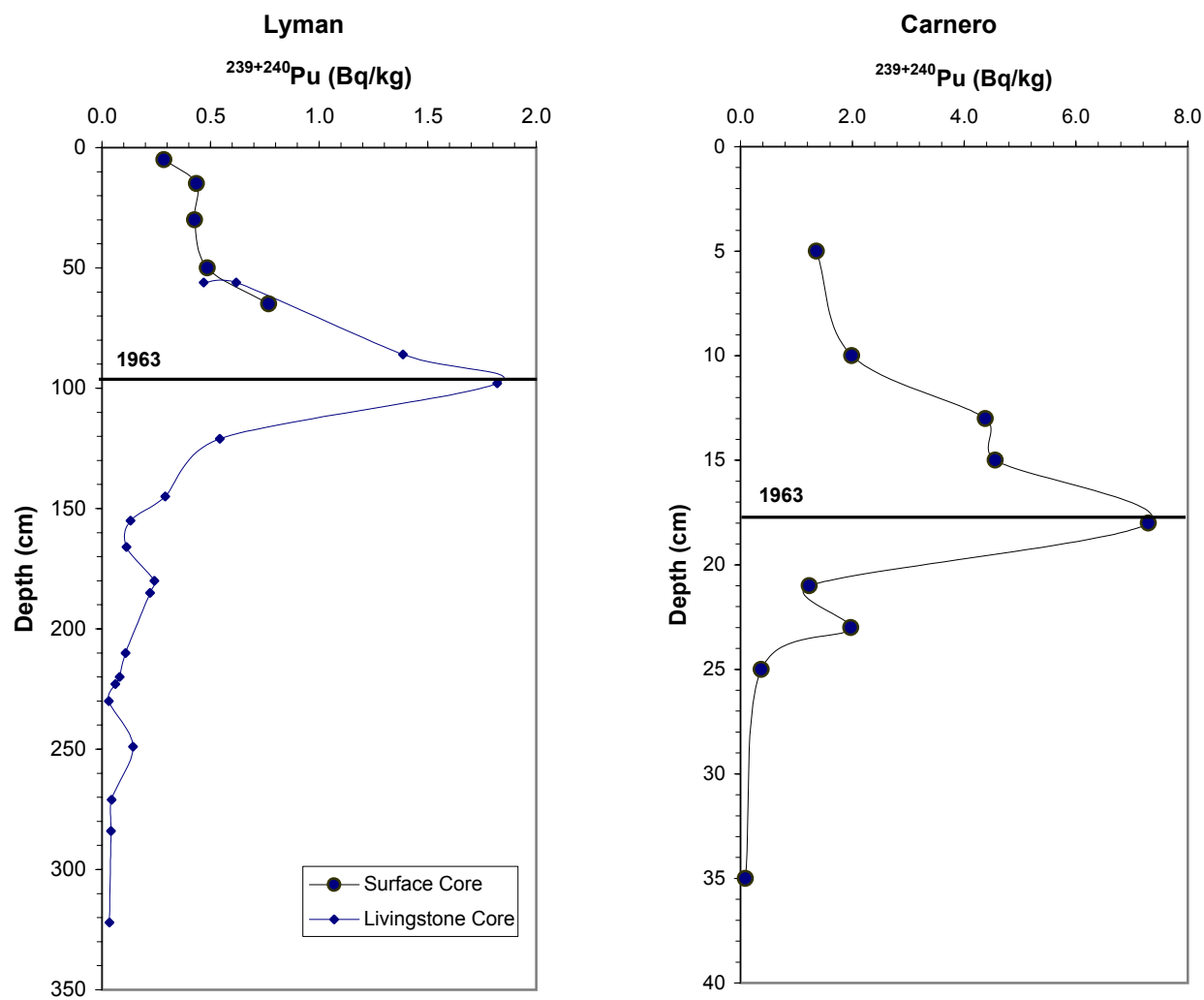


Figure 3b. Plutonium activity for Lyman and Carnero Lakes.

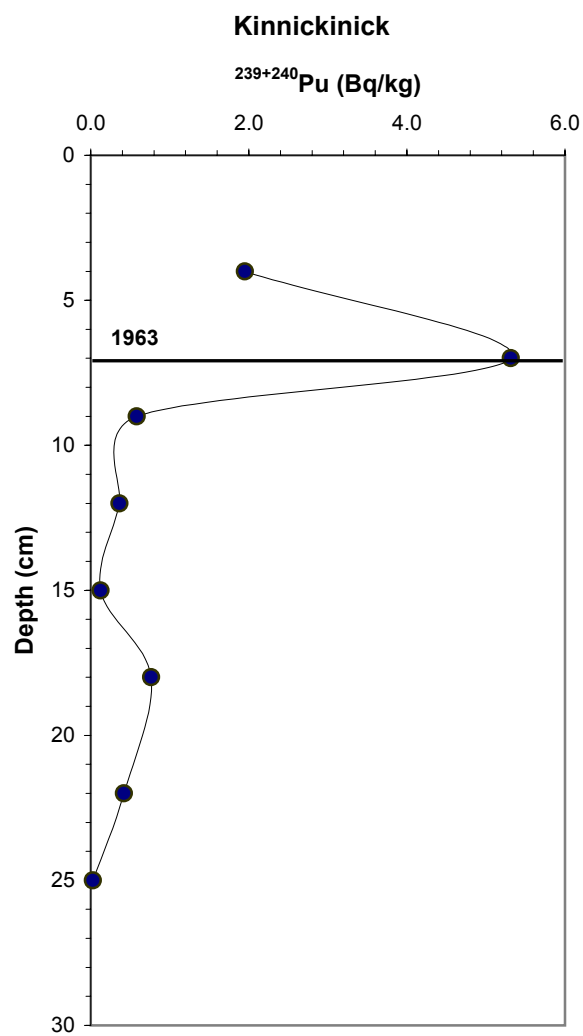


Figure 3c. Plutonium activity for Kinnickinick Lake.

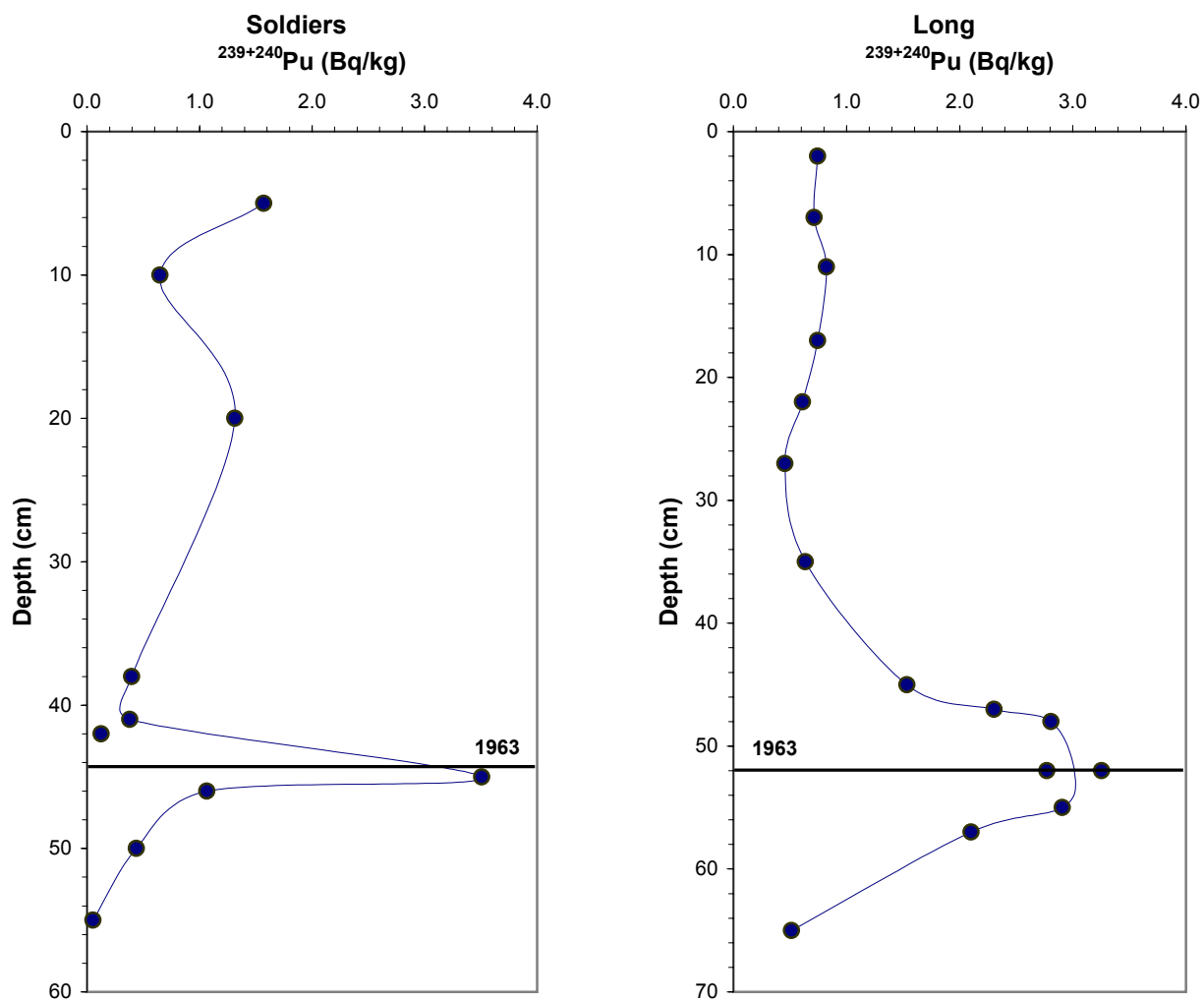


Figure 3d. Plutonium activity for Soldiers and Long Lakes.

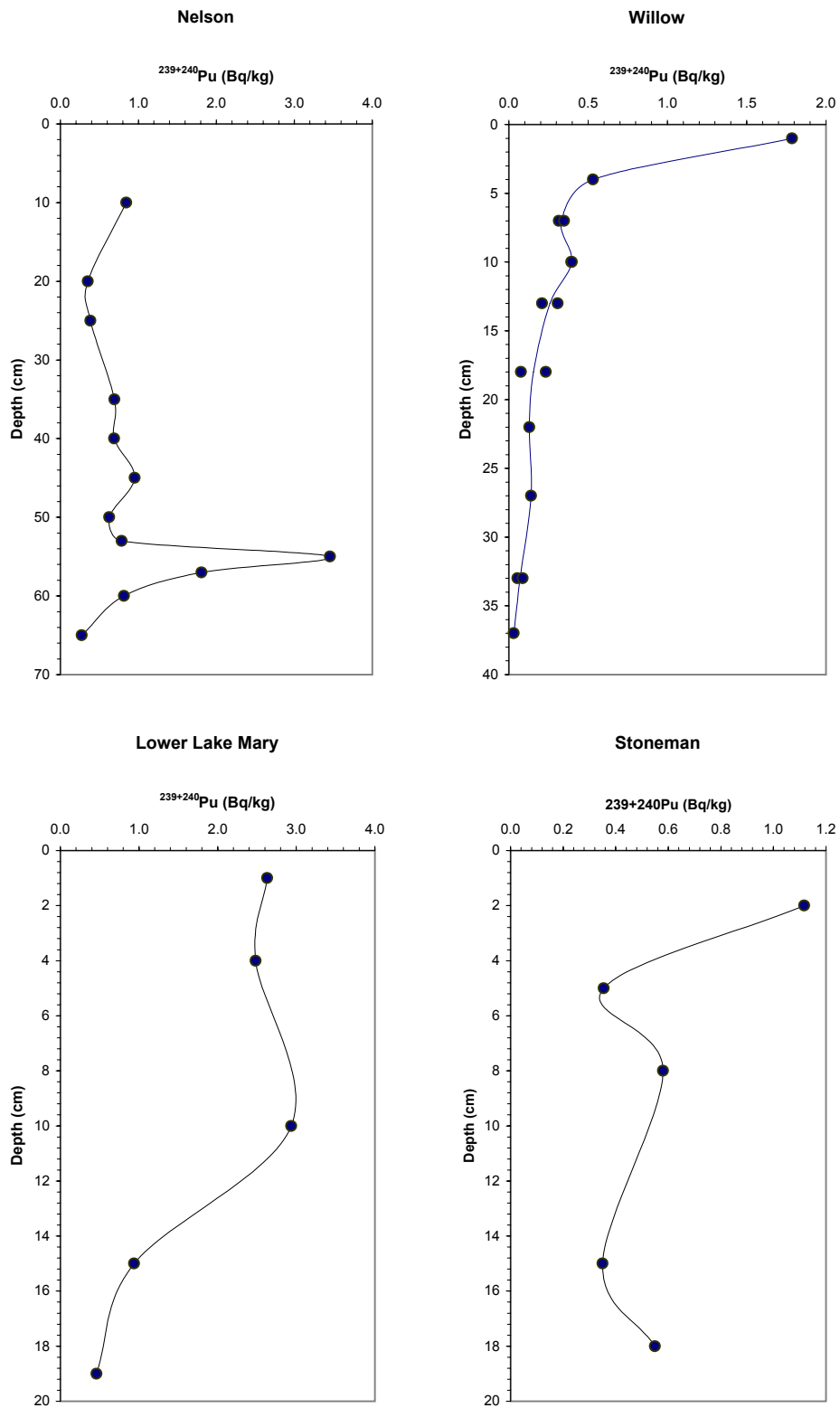


Figure 3e. Plutonium activity for Nelson, Willow Springs, Lower Lake Mary, and Stoneman.

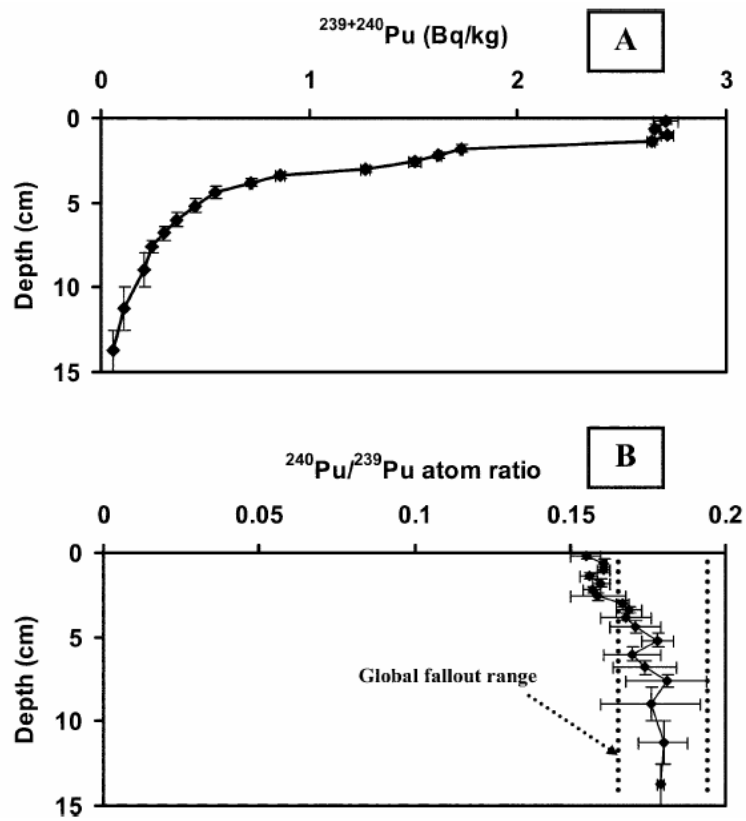


Figure 4. Lockett Meadow, Arizona soil depth profiles. From Ketterer et al., 2003.

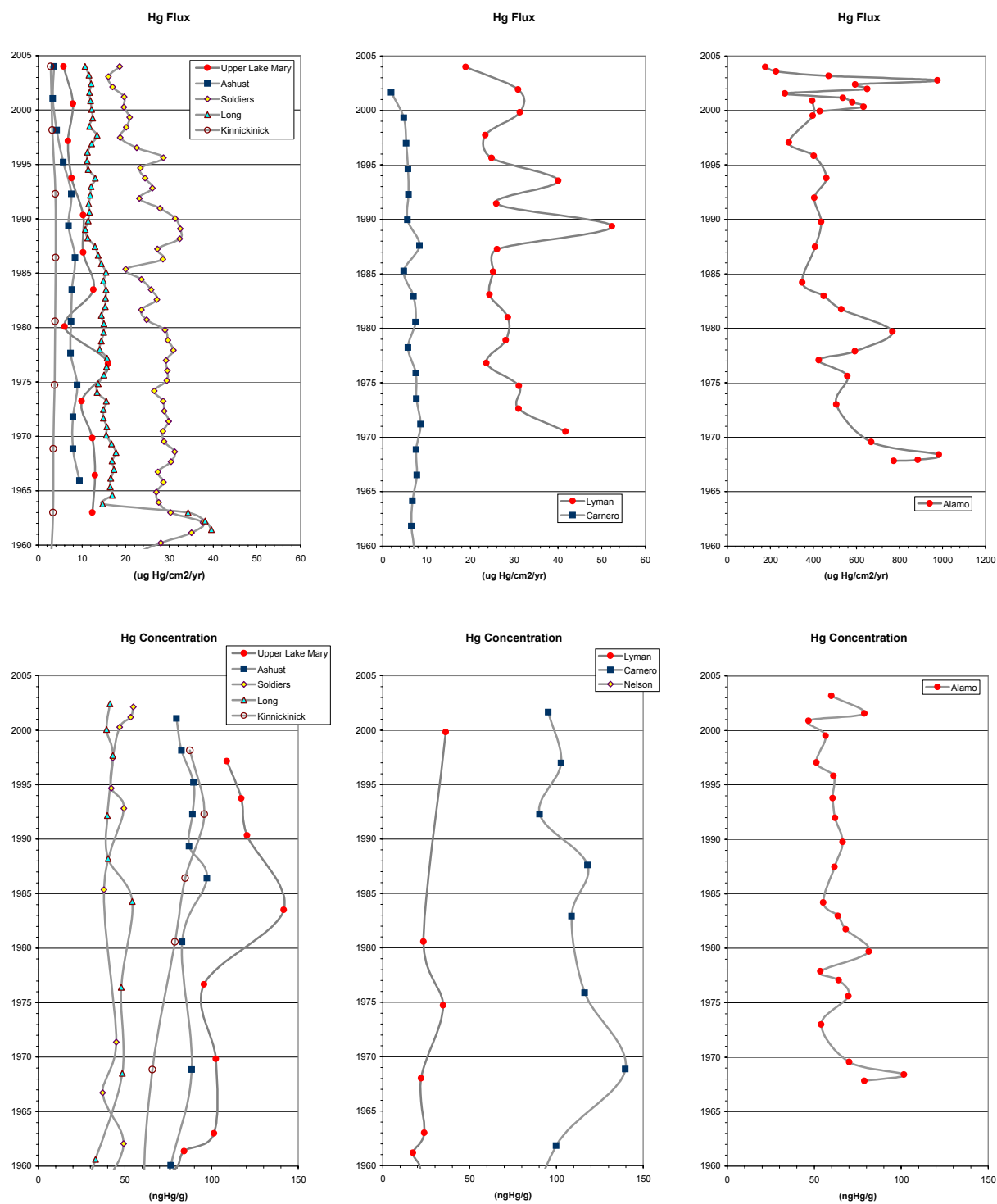


Figure 5a. Mercury flux (top) and concentration (bottom) in post-1963 sediments.

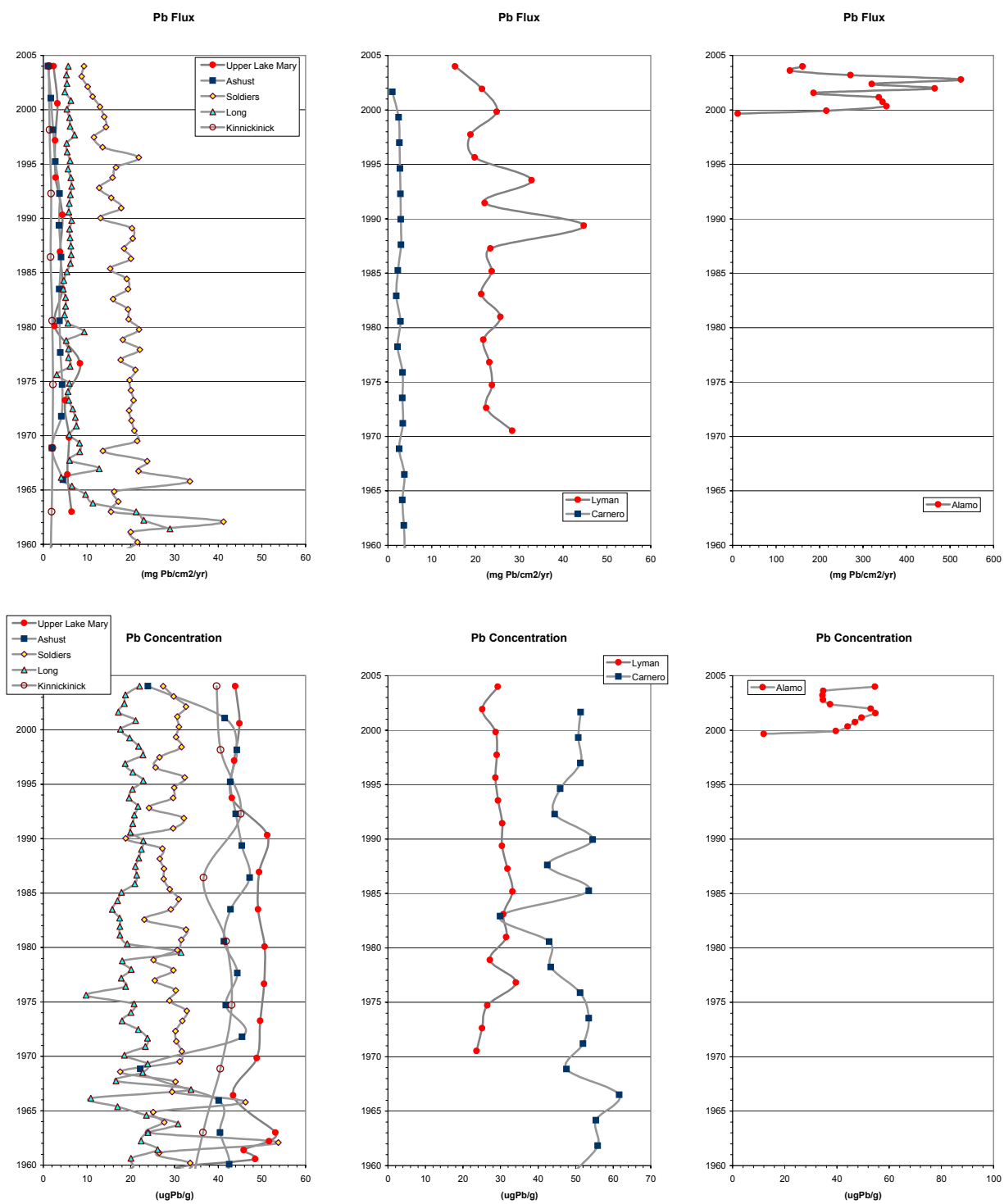


Figure 5b. Lead flux (top) and concentration (bottom) in post-1963 sediments.

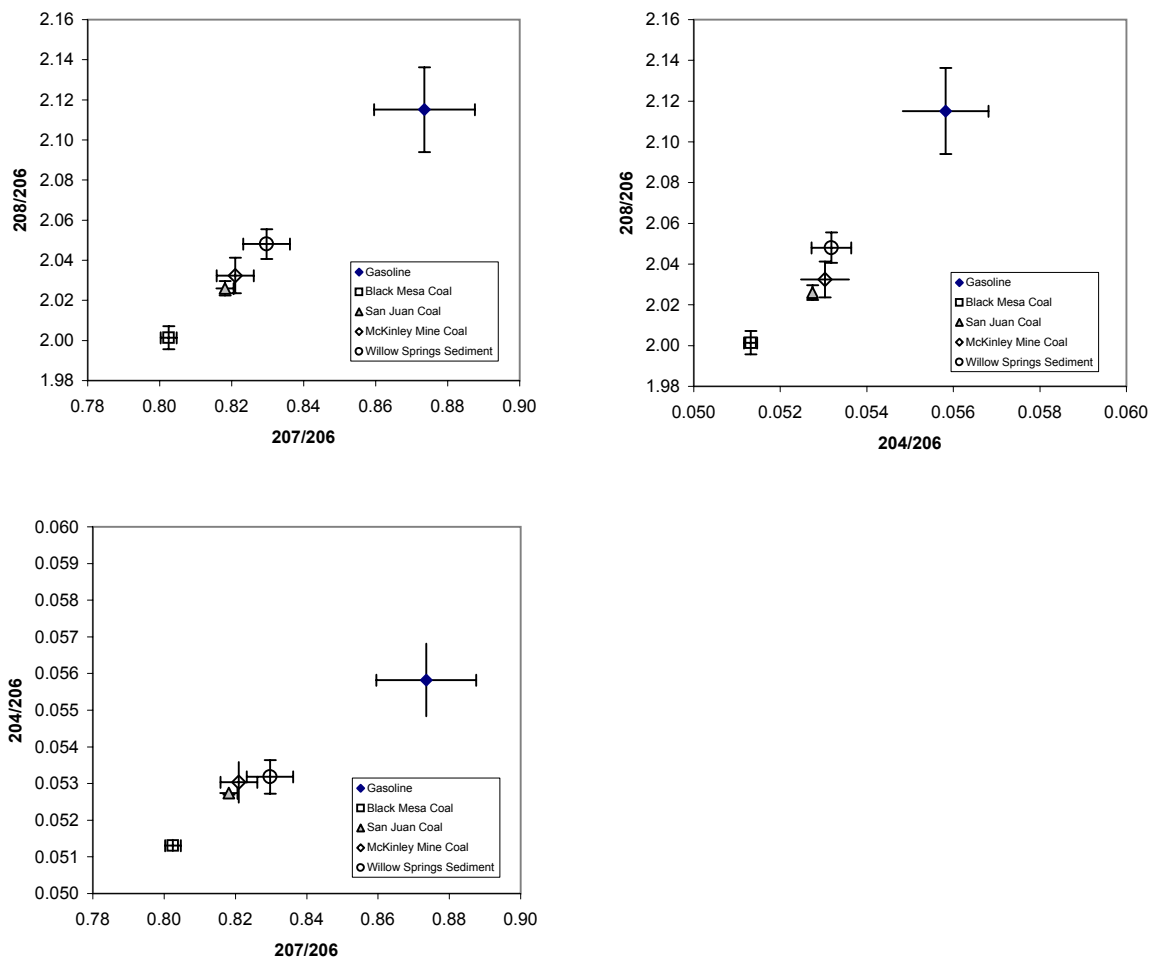


Figure 6a. Pb stable isotope ratios for coal and gasoline potential end members and for Willow Springs Sediments.

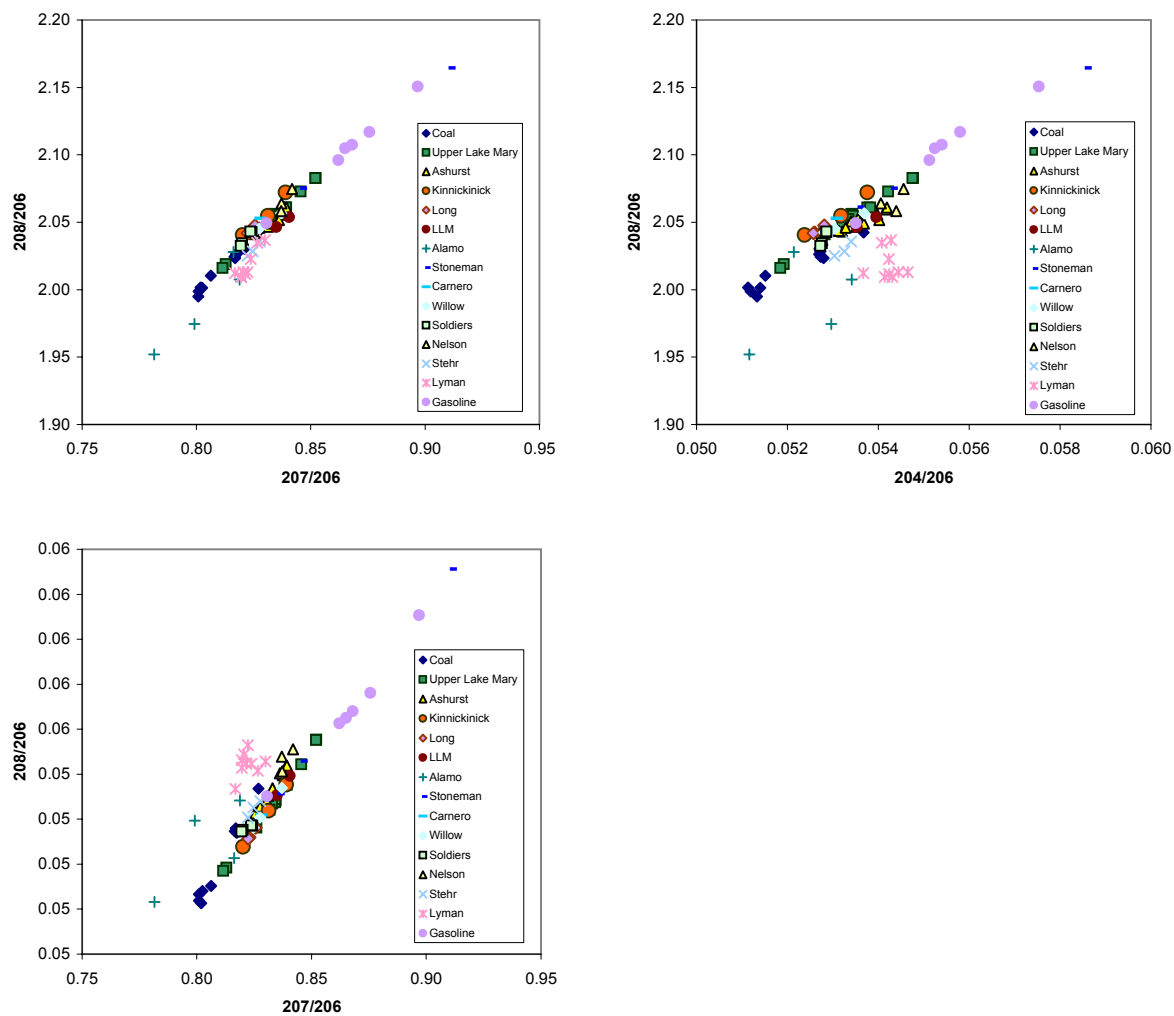


Figure 6b. Pb stable isotope ratios lake sediments and potential end members.

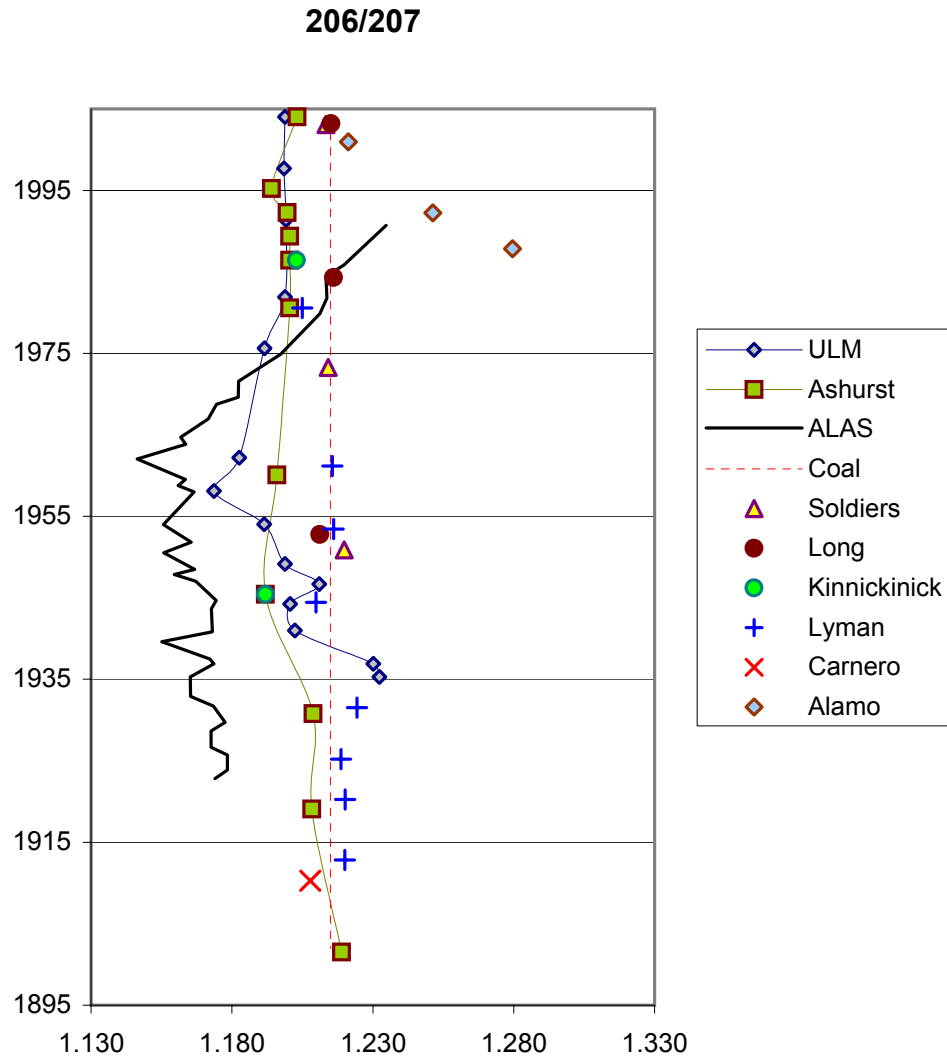


Figure 7. Pb isotope ratio 206/207 versus year for the potential end members and lake sediments.

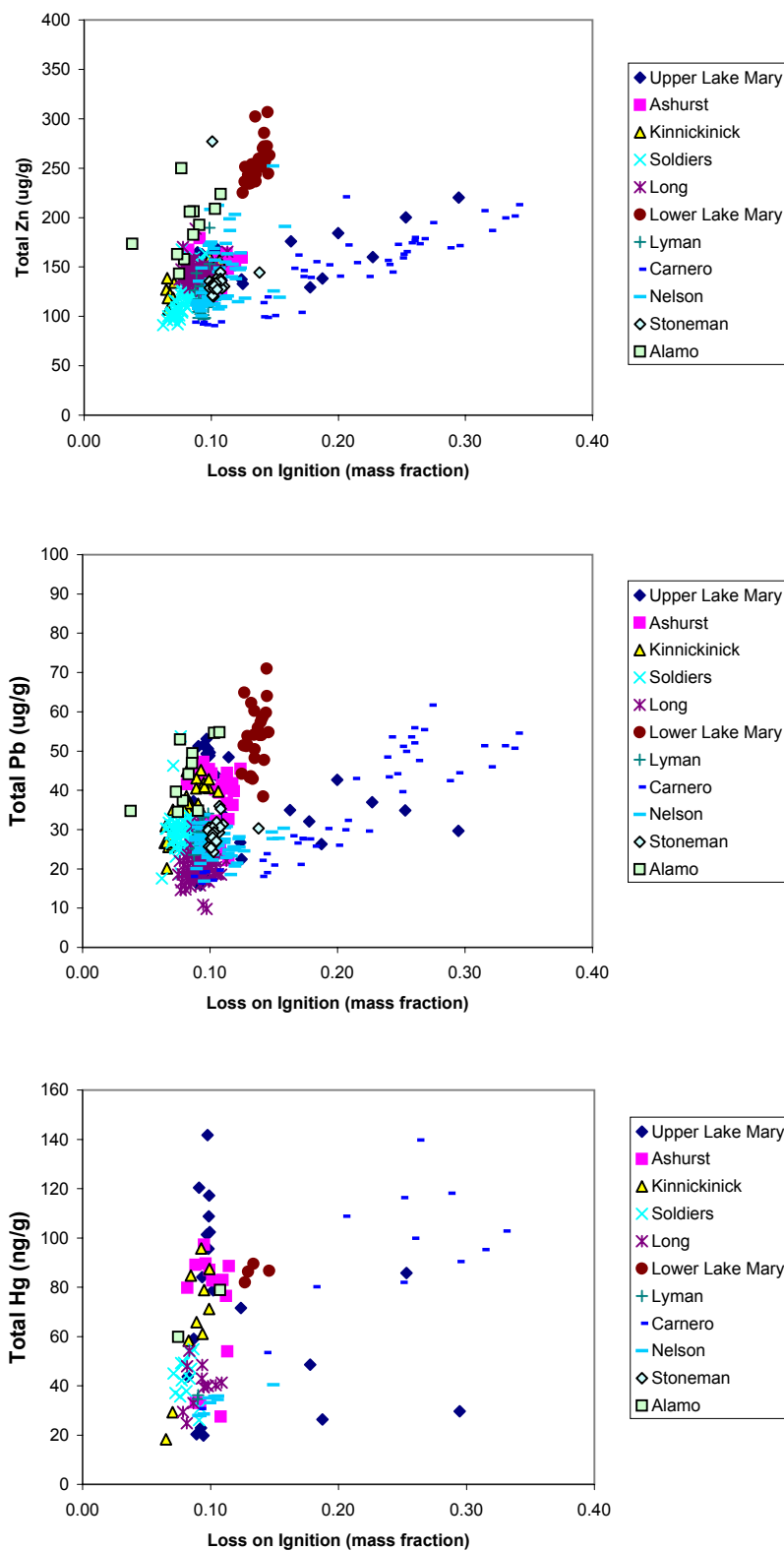


Figure 8. Metals concentrations in lake sediment versus loss-on-ignition.

Table 1. Reservoir Summary

Reservoir	Area (acres)	Average depth (ft)	Elevation (ft)	Year Impounded
Upper Lake Mary	600	38	6,895	1941
Kinnickinick Lake	229	12	7,100	1954
Soldier Lake	126	22	7,040	n/a
Long Lake	268	<1 (presently)	6,700	n/a
Lower Lake Mary	n/a	3	6,800	1904
Lyman Lake	1,400	22	5,980	1915
Carnero Lake	n/a	14	9,000	1979
Nelson Reservoir	60	15	7,410	1892
Stoneman Lake	n/a	0 (presently)	n/a	Natural
Willow Springs Lake	150	60	7,520	1967
Alamo Lake	n/a	n/a	n/a	1968

Sources: Arizona Game and Fish Department Region I Office, Pinetop, AZ and Region II Office, Flagstaff, AZ.

Table 2. Age Models and Estimated Average Sedimentation Rates

Sedimentation Rates					
Lake	Age Marker	Accumulation (cm)	Time (yr)	Rate (cm/yr)	Depth Range (cm)
Upper Lake Mary	1963 = 12cm	12	41	0.29	0 to 12 cm
	1941 = 39cm	27	22	1.23	12 to 46 cm
Ashurst	1963 = 14cm	14	41	0.34	0 to 36 cm
Kinnickinick	1963 = 7cm	7	41	0.17	0 to 26 cm
Soldiers	1963 = 44cm	44	41	1.07	0 to 59 cm
Long	1963 = 52cm	52	41	1.27	0 to 69 cm
Lyman	1963 = 98cm	98	41	2.39	0 to 98 cm
	1910 = 475cm	377	53	7.11	98 to 475 cm
Lower Lake Mary	No Model				0 to 25 cm
Carnero	1963 = 17.5cm	17.5	41	0.43	0 to 44 cm
Nelson	No Model				0 to 69 cm
Willow Springs	No Model				0 to 38 cm
Stoneman	No Model				0 to 21
Alamo	1968 = 440cm	440	36	12.22	0 to 440 cm

Table 3. Comparison of Flux and Parameters Used to Calculate Flux for 1960 to 1965 and 1999 to 2004.

Lake	Bulk Density		Sedimentation Rate		Hg Concentration		Hg Flux		Pb Concentration		Pb Flux	
	(g/cm ³)		(g/cm ² /yr)		(ng/g)		(ng/cm ² /yr)		(ug/g)		(ug/cm ² /yr)	
	1960 to 1965	1999 to 2004	1960 to 1965	1999 to 2004	1960 to 1965	1999 to 2004	1960 to 1965	1999 to 2004	1960 to 1965	1999 to 2004	1960 to 1965	1999 to 2004
Upper Lake Mary	0.504	0.214	0.522	0.063	92.74	108.81	44.84	6.83	49.78	44.15	25.44	2.77
Ashurst	0.307	0.127	0.105	0.043	76.48	79.79	8.47	3.46	41.05	32.76	4.30	1.41
Kinnickinick	0.309	0.188	0.053	0.032	63.46	87.42	3.35	2.81	36.55	39.66	1.93	1.27
Soldiers	0.639	0.339	0.686	0.364	49.18	51.64	30.61	18.61	33.84	30.33	23.60	11.05
Long	0.592	0.229	0.751	0.290	32.98	40.38	27.91	11.79	23.42	19.28	17.46	5.58
Lyman	0.453	0.313	2.720	0.747	20.90	36.18	54.22	27.04	.	27.71	.	20.54
Carnero	0.157	0.081	0.067	0.034	99.78	95.27	6.83	3.37	53.72	51.03	3.58	1.75
Alamo	n/a	0.575	n/a	7.102	n/a	69.37	n/a	504.20	n/a	43.97	n/a	301.04

Table 4. Average concentrations of Hg, Pb, and Zn in lake sediments.

Lake	n	Hg (ng/g)		n	Pb (ug/g)		n	Zn (ug/g)	
		Mean	Std. Dev.		Mean	Std. Dev.		Mean	Std. Dev.
Upper Lake Mary	20	70.99	37.98	47	40.56	26.67	47	196.0	236.7
Ashurst	13	70.86	24.77	37	34.31	8.14	37	142.7	15.9
Kinnickinick	10	65.07	24.91	27	35.48	6.52	27	140.6	14.0
Soldiers	13	42.38	8.59	60	29.25	5.13	60	118.7	19.1
Long	11	40.15	8.59	69	20.22	3.91	70	145.0	9.4
Lower Lake Mary	4	86.07	3.14	26	53.70	7.72	26	255.8	19.9
Lyman	16	23.09	5.61	17	29.10	2.89	17	120.5	24.3
Carnero	12	93.10	29.36	44	36.04	14.00	44	150.1	37.0
Nelson	9	33.17	4.30	70	26.62	3.26	70	137.2	31.3
Willow Springs	9	38.98	34.64	39	27.54	17.92	39	70.2	20.8
Stoneman	n/a	n/a	n/a	22	30.27	5.75	22	159.9	102.8
Alamo	21	64.99	12.42	11	43.97	8.19	11	191.6	31.4
Surface	24	79.97	26.29	61	39.32	16.28	61	166.4	76.0
Core Base	12	35.72	22.46	10	22.93	8.09	10	159.8	63.8

Notes: n/a = No samples analyzed.

Samples were not analyzed for Pb or Zn at the base of Lyman or Alamo cores.

Surface samples are the average of the top 4 cm of sample, base samples are the single observation at the lowest point in each core

Table 5. Pb Stable Isotope Analysis of Potential End Members.

Chow and Johnstone 1965 Gasoline				
Sample	204/206	207/206	208/206	
Wilshire D	0.055127	0.862069	2.09599665	
Wilshire Regular	0.055249	0.865052	2.10482004	
Douglas	0.055402	0.868056	2.10748156	
Standard Oil Regular	0.055804	0.875657	2.11685013	
Shell Oil Regular	0.057537	0.896861	2.15053763	
1947 Tetraethyl Lead	0.053505	0.830565	2.04918033	
NAU Analyses				
Sample	204/206	207/206	208/206	
Black Mesa 1	0.051191	0.800935	1.99868773	
Black Mesa 2	0.051134	0.801832	2.00152727	
Black Mesa 3	0.051329	0.800842	1.99498943	
Black Mesa 4	0.051512	0.806266	2.01045717	
Black Mesa 5	0.051401	0.802489	2.0014383	
San Juan 1	0.052704	0.820926	2.03018897	
San Juan 2	0.052795	0.816939	2.0234464	
San Juan 3	0.052732	0.816588	2.02442787	
McKinley Mine 1	0.053676	0.826863	2.04249197	
McKinley Mine 2	0.052726	0.818679	2.02841067	
McKinley Mine 3	0.052697	0.817354	2.02635513	
Pre-impoundment Soil (Willow Springs Sediment)				
Sample	204/206	207/206	208/206	
0-1 cm	0.053692	0.837039	2.05653997	
20-21 cm	0.05304	0.827487	2.04529663	
35-36 cm	0.05281	0.824548	2.0424113	
Statistics: 204/206				
	N	Mean	Stdev	RSD
Gasoline*	5	0.055824	0.00099142	1.78
Black Mesa Coal	5	0.051313	0.00015392	0.30
San Juan Coal	3	0.052744	4.7013E-05	0.09
McKinley Mine Coal	3	0.053033	0.00055704	1.05
Willow Springs	3	0.053181	0.00045748	0.86
Statistics: 207/206				
	N	Mean	Stdev	RSD
Gasoline*	5	0.873539	0.01398267	1.60
Black Mesa Coal	5	0.802473	0.00222606	0.28
San Juan Coal	3	0.818151	0.00240982	0.29
McKinley Mine Coal	3	0.820965	0.00515008	0.63
Willow Springs	3	0.829691	0.00653061	0.79
Statistics: 208/206				
	N	Mean	Stdev	RSD
Gasoline*	5	2.115137	0.02113964	1.00
Black Mesa Coal	5	2.00142	0.00571182	0.29
San Juan Coal	3	2.026021	0.0036427	0.18
McKinley Mine Coal	3	2.032419	0.00878356	0.43
Willow Springs	3	2.048083	0.007465	0.36

Notes: Gasoline statistics do not include 1947 sample.

Table 6. Comparison of Surface Sediment Hg Collected and Analyzed by ADEQ versus NAU.

	Upper Lake Mary	Lower Lake Mary	Willow Springs	Soldier
ADEQ Surface Sediment Hg (ng/g)				
	28.20	61.80	73.80	35.59
	29.63	65.00		
	34.70	72.50		
	37.97	80.29		
	40.90			
	43.24			
	44.30			
	46.15			
	50.30			
	76.60			
	80.92			
	80.92			
n	12	4	1	1
Mean	49.49	69.90	73.80	35.59
Std. Dev.	19.22	8.25		
RSD	39%	12%		
NAU Surface Sediment Hg (ng/g)				
	108.81	81.91	127.11	54.78
	117.14		55.06	53.25
	120.44		24.62	46.89
n	3	1	3	3
Mean	115.46	81.91	68.93	51.64
Std. Dev.	3.34		3.34	3.34
RSD	3%		5%	6%

Appendix A.

Quality Assurance Project Plan

Submitted as a separate PDF File

Anderson Mesa**Upper Lake Mary**

Depth (cm)	Moisture (wt f)	Bulk density (g/cc)	Loss on Ignition (wt f)	Zinc (mg/kg)	Total Pb (mg/kg)	Hg (ng/g)	Pb Isotope Mass Ratio 204/206	Pb Isotope Mass Ratio 207/206	Pb Isotope Mass Ratio 208/206	Plutonium 239+240 (Bq/kg)
0	0.837	0.182	0.104	168.3	43.90		0.05343	0.83418	2.0562	0.7405
1	0.784	0.249	0.093	163.0	44.87					
2	0.810	0.213	0.099	155.2	43.69	108.81	0.05341	0.83440	2.0559	
3	0.806	0.222	0.099	137.2	43.16	117.14				
4	0.755	0.292	0.091	142.2	51.25	120.44	0.05338	0.83388	2.0530	
5	0.760	0.267	0.097	140.2	49.36					
6	0.735	0.304	0.098	139.1	49.14	141.68				1.7451
7	0.715	0.174	0.098	136.3	50.63		0.05337	0.83414	2.0515	1.9663
8	0.564	0.570	0.098	151.2	50.51	95.60				2.4551
9	0.711	0.342	0.100	149.3	49.63		0.05376	0.83921	2.0609	3.2713
10	0.643	0.413	0.099	149.8	48.84	102.42				3.3488
11	0.646	0.435	0.099	151.5	43.45					4.8994
12	0.660	0.417	0.097	153.5	53.12	101.37				5.0052
13	0.664	0.399	0.095	150.5	51.68		0.05422	0.84558	2.0728	6.5515
14	0.620	0.470	0.094	141.5	45.85	84.11				4.4990
15	0.493	0.732	0.115	148.7	48.47					2.8613
16	0.446	0.823	0.102	168.2	30.42	78.69				1.4506
17	0.430	0.864	0.098	161.0	48.57					1.9499
18	0.395	0.945	0.087	143.3	37.20	59.05	0.05476	0.85206	2.0828	0.2720
19	0.379	0.979	0.080	138.1	35.87					0.1930
20	0.386	0.948	0.089	142.7	36.43					
21	0.351	0.999	0.084	149.1	28.75					0.2976
22	0.336	1.084	0.081	133.1	25.91					0.2031
23	0.324	1.059	0.079	125.5	29.97		0.05382	0.83932	2.0609	
24	0.302	1.145	0.082	133.4	23.90	43.65				
25	0.319	1.134	0.086	131.2	30.62					
26	0.348	1.048	0.097	146.7	28.52					
27	0.349	1.053	0.111	162.7	33.52					0.0757
28	0.481	0.682	0.163	175.8	34.98					
29	0.537	0.611	0.200	184.4	42.68		0.05344	0.83419	2.0547	
30	0.345	1.002	0.103	121.9	29.15					0.0302
31	0.386	0.966	0.108	136.3	25.24					
32	0.407	0.905	0.124	137.3	26.69	71.53	0.05282	0.82581	2.0413	
33	0.406	0.881	0.125	132.8	22.45					
34	0.631	0.448	0.253	200.2	34.91	85.77				
35	0.624	0.416	0.227	160.1	36.93		0.05335	0.83285	2.0524	
36	0.549	0.589	0.178	129.5	32.12	48.58				0.0898
37	0.652	0.410	0.295	220.3	29.69	29.67				
38	0.799	0.222	0.695	1585.2	123.58	42.01				
39	0.803	0.188	0.707	925.5	178.46		0.05321	0.83170	2.0488	
40	0.455	0.753	0.187	138.5	26.33	26.33				
41	0.308	1.136	0.096	143.5	18.16					
42	0.283	1.143	0.093	137.5	15.88	22.83				0.0904
43	0.303	1.118	0.094	144.2	18.53					
44	0.276	1.054	0.094	139.5	19.87	19.75	0.05192	0.81291	2.0189	
45	0.285	1.065	0.089	123.1	17.20					0.0271
46	0.265	1.078	0.089	164.9	16.41	20.37	0.05185	0.81151	2.0162	

Ashurst Lake

Depth (cm)	Moisture (wt f)	Bulk density (g/cc)	Loss on Ignition (wt f)	Zinc (mg/kg)	Total Pb (mg/kg)	Hg (ng/g)	Pb Isotope Mass Ratio 204/206	Pb Isotope Mass Ratio 207/206	Pb Isotope Mass Ratio 208/206	Plutonium 239+240 (Bq/kg)
0	0.874	0.132	0.091	179.1	23.96		0.05352	0.83116	2.0467	

Depth (cm)	Moisture (wt f)	Bulk density (g/cc)	Loss on Ignition (wt f)	Zinc (mg/kg)	Total Pb (mg/kg)	Hg (ng/g)	Pb Isotope Mass Ratio 204/206	Pb Isotope Mass Ratio 207/206	Pb Isotope Mass Ratio 208/206	Plutonium 239+240 (Bq/kg)
1	0.880	0.122	0.082	167.4	41.55	79.79				
2	0.856	0.148	0.101	158.0	44.28	82.71				7.2938
3	0.813	0.187	0.096	142.0	42.77	89.57	0.05398	0.83750	2.0556	
4	0.775	0.249	0.088	143.7	44.05	89.02	0.05355	0.83361	2.0529	1.5832
5	0.784	0.232	0.099	146.0	45.43	87.06	0.05365	0.83300	2.0502	
6	0.769	0.253	0.095	146.4	47.23	97.31	0.05361	0.83298	2.0502	
7	0.769	0.250	0.092	143.6	42.84					2.3585
8	0.759	0.265	0.109	151.2	41.32	82.95	0.05368	0.83297	2.0490	
9	0.761	0.256	0.113	148.4	44.39					
10	0.734	0.303	0.118	158.1	41.78					3.6177
11	0.761	0.266	0.124	159.3	45.50					
12	0.763	0.262	0.115	155.9	22.19	88.51				
13	0.713	0.326	0.104	153.2	40.17					
14	0.727	0.311	0.116	153.9	40.45					5.9709
15	0.744	0.285	0.112	163.4	42.53	76.48	0.05402	0.83614	2.0517	4.1723
16	0.678	0.382	0.107	154.9	39.36					5.1271
17	0.703	0.345	0.119	155.8	39.76					4.2394
18	0.633	0.450	0.118	155.2	36.25					
19	0.529	0.628	0.115	151.4	32.65					1.2638
20	0.513	0.671	0.113	155.7	36.74	53.95	0.05418	0.83898	2.0603	
21	0.481	0.731	0.104	147.0	32.25					
22	0.460	0.777	0.097	139.4	31.99					
23	0.434	0.857	0.091	134.9	29.32					
24	0.402	0.925	0.089	122.0	25.58		0.05325	0.82728	2.0457	
25	0.388	0.930	0.088	129.3	26.39	33.29				0.0753
26	0.380	0.935	0.092	125.3	27.88	32.98				
27	0.374	0.964	0.090	120.3	26.34					
28	0.374	0.951	0.094	118.4	26.04					
29	0.378	0.957	0.096	117.3	26.53					
30	0.378	0.962	0.095	129.4	29.17		0.05328	0.82756	2.0459	0.0766
31	0.366	0.972	0.101	120.6	24.31					
32	0.375	0.973	0.101	120.6	26.77					
33	0.354	1.011	0.094	130.1	27.20					
34	0.384	0.950	0.105	125.9	23.90					
35	0.375	0.977	0.108	125.2	25.65	27.52	0.05277	0.82040	2.0368	
36	0.375	0.963	0.097	130.6	25.05					

Kinnickinick Lake

Depth (cm)	Moisture (wt f)	Bulk density (g/cc)	Loss on Ignition (wt f)	Zinc (mg/kg)	Total Pb (mg/kg)	Hg (ng/g)	Pb Isotope Mass Ratio 204/206	Pb Isotope Mass Ratio 207/206	Pb Isotope Mass Ratio 208/206	Plutonium 239+240 (Bq/kg)
0	0.821	0.188	0.106	157.2	39.66					
1	0.801	0.212	0.099	150.0	40.57	87.42				
2	0.783	0.237	0.093	143.4	45.16	95.75				
3	0.754	0.272	0.085	136.8	36.67	84.77	0.05319	0.83134	2.0546	
4	0.748	0.284	0.095	130.6	41.83	78.82				1.9516
5	0.739	0.302	0.089	142.1	43.09					
6	0.731	0.303	0.089	150.4	40.49	65.79				
7	0.719	0.309	0.091	145.5	36.55					5.3157
8	0.757	0.267	0.094	148.0	34.53	61.13				
9	0.767	0.251	0.096	149.8	40.89					0.5838
10	0.758	0.273	0.099	159.6	42.84	71.16	0.05376	0.83901	2.0722	
11	0.735	0.294	0.082	154.9	44.89					
12	0.730	0.311	0.084	151.7	37.08					0.3645

Depth (cm)	Moisture (wt f)	Bulk density (g/cc)	Loss on Ignition (wt f)	Zinc (mg/kg)	Total Pb (mg/kg)	Hg (ng/g)	Pb Isotope Mass Ratio 204/206	Pb Isotope Mass Ratio 207/206	Pb Isotope Mass Ratio 208/206	Plutonium 239+240 (Bq/kg)
13	0.725	0.319	0.082	150.3	38.53					
14	0.659	0.322	0.084	153.2	36.41					
15	0.844	0.343	0.083	154.4	34.92	58.26				0.1246
16	0.676	0.351	0.083	147.2	36.72					
17	0.679	0.337	0.083	145.7	32.34					
18	0.667	0.377	0.080	141.2	34.99					0.7650
19	0.645	0.438	0.071	134.1	35.05					
20	0.473	0.759	0.065	127.0	26.62					
21	0.423	0.859	0.068	122.8	25.61					
22	0.394	0.925	0.070	117.9	26.13	29.31				0.4218
23	0.368	0.989	0.070	118.9	28.56					
24	0.353	1.046	0.066	118.5	26.67					
25	0.347	1.046	0.065	138.6	30.89	18.31	0.05239	0.82019	2.0404	0.0293
26	0.347	1.027	0.066	107.0	20.16					

Soldier's Lake

Depth (cm)	Moisture (wt f)	Bulk density (g/cc)	Loss on Ignition (wt f)	Zinc (mg/kg)	Total Pb (mg/kg)	Hg (ng/g)	Pb Isotope Mass Ratio 204/206	Pb Isotope Mass Ratio 207/206	Pb Isotope Mass Ratio 208/206	Plutonium 239+240 (Bq/kg)
0	0.717	0.316	0.089	134.7	27.45		0.05286	0.82414	2.0426	1.5700
1	0.753	0.273	0.088	133.6	29.83					
2	0.739	0.289	0.087	159.6	32.65	54.78				
3	0.705	0.343	0.085	125.7	30.68	53.25				
4	0.668	0.389	0.085	123.6	31.04	46.89				
5	0.647	0.427	0.082	122.7	30.34					
6	0.649	0.423	0.080	126.3	31.59					
7	0.655	0.406	0.084	120.8	26.59	42.92				
8	0.598	0.492	0.081	108.6	25.65					
9	0.538	0.629	0.075	101.0	32.36					
10	0.588	0.517	0.077	105.3	29.96	42.11				0.6493
11	0.597	0.498	0.072	107.2	29.67					
12	0.612	0.493	0.079	112.6	24.17	49.34				
13	0.628	0.449	0.082	115.5	32.19					
14	0.567	0.559	0.075	106.7	29.68					
15	0.525	0.649	0.077	103.8	18.82					
16	0.500	0.694	0.073	92.2	27.27					
17	0.491	0.716	0.070	96.2	26.65					
18	0.525	0.624	0.075	96.8	27.61					
19	0.503	0.677	0.071	97.7	27.54					
20	0.599	0.492	0.081	116.9	28.95	37.79				1.3136
21	0.555	0.574	0.084	114.6	30.93					
22	0.540	0.620	0.073	107.6	29.17					
23	0.516	0.644	0.073	107.5	23.11					
24	0.580	0.553	0.085	117.7	32.63					
25	0.557	0.575	0.082	115.6	31.55					
26	0.509	0.665	0.078	120.2	30.65					
27	0.506	0.672	0.073	102.6	25.21					
28	0.504	0.692	0.072	109.4	29.77					
29	0.524	0.647	0.073	103.9	25.48					
30	0.526	0.647	0.071	99.0	30.32					
31	0.532	0.637	0.069	104.0	28.85					
32	0.565	0.568	0.069	102.7	32.83					
33	0.547	0.605	0.068	101.7	31.79		0.05286	0.82365	2.0432	
34	0.544	0.604	0.066	100.1	30.25					

Depth (cm)	Moisture (wt f)	Bulk density (g/cc)	Loss on Ignition (wt f)	Zinc (mg/kg)	Total Pb (mg/kg)	Hg (ng/g)	Pb Isotope Mass Ratio 204/206	Pb Isotope Mass Ratio 207/206	Pb Isotope Mass Ratio 208/206	Plutonium 239+240 (Bq/kg)
35	0.537	0.618	0.071	99.9	30.39	44.93				
36	0.549	0.613	0.073	106.7	31.67					
37	0.530	0.641	0.070	101.3	31.22					
38	0.481	0.723	0.062	91.0	17.56					0.3970
39	0.479	0.733	0.065	96.1	30.24					
40	0.506	0.688	0.073	115.1	29.48	37.05				
41	0.506	0.676	0.071	116.0	46.26					0.3800
42	0.533	0.601	0.082	122.6	25.14					0.1268
43	0.554	0.579	0.086	125.6	27.64					
44	0.528	0.603	0.083	115.2	23.95					
45	0.471	0.714	0.077	124.6	53.77	49.18				3.5072
46	0.492	0.703	0.080	117.7	26.52					1.0649
47	0.547	0.597	0.084	124.1	33.60					
48	0.589	0.519	0.083	157.9	32.66					
49	0.562	0.547	0.077	127.3	31.71					
50	0.531	0.603	0.076	121.9	30.49	35.65				0.4390
51	0.581	0.539	0.080	127.6	28.71					
52	0.614	0.496	0.083	138.0	28.14					
53	0.630	0.450	0.091	139.4	28.11					
54	0.622	0.433	0.085	145.2	26.80					
55	0.634	0.440	0.091	154.9	28.22	26.02				0.0540
56	0.626	0.452	0.095	163.8	25.84					
57	0.550	0.590	0.088	147.4	23.99		0.05274	0.81975	2.0334	
58	0.570	0.544	0.092	158.4	24.21	31.05				
59	0.393	0.912	0.077	167.8	25.44					

Long Lake

Depth (cm)	Moisture (wt f)	Bulk density (g/cc)	Loss on Ignition (wt f)	Zinc (mg/kg)	Total Pb (mg/kg)	Hg (ng/g)	Pb Isotope Mass Ratio 204/206	Pb Isotope Mass Ratio 207/206	Pb Isotope Mass Ratio 208/206	Plutonium 239+240 (Bq/kg)
0	0.814	0.204	0.113	165.3	22.05		0.05260	0.82292	2.0424	0.7436
1	0.799	0.221	0.104	154.3	18.76					
2	0.791	0.230	0.109	146.5	18.56	41.34				
3	0.794	0.227	0.097	150.5	17.15					
4	0.788	0.235	0.096	147.9	21.11					
5	0.781	0.243	0.095	140.3	17.62	39.42				
6	0.787	0.241	0.100	138.4	19.72					
7	0.779	0.221	0.095	141.7	21.77					0.7141
8	0.775	0.247	0.093	142.6	22.78	43.00				
9	0.792	0.226	0.106	137.9	18.71					
10	0.803	0.210	0.105	146.0	20.45					
11	0.802	0.211	0.100	147.5	22.88					0.8217
12	0.798	0.218	0.083	140.5	20.42					
13	0.770	0.252	0.087	137.1	19.64					
14	0.789	0.236	0.097	139.1	21.65					
15	0.786	0.235	0.098	140.3	20.81	39.81				
16	0.790	0.228	0.096	136.9	20.49					
17	0.786	0.231	0.095	139.1	19.92					0.7455
18	0.797	0.224	0.094	141.6	22.86					
19	0.802	0.211	0.104	141.0	22.45					
20	0.792	0.221	0.104	141.3	21.84	40.27				
21	0.782	0.237	0.093	138.5	21.06					
22	0.782	0.235	0.098	145.3	21.38					0.6121
23	0.786	0.233	0.090	144.4	20.93					

Depth (cm)	Moisture (wt f)	Bulk density (g/cc)	Loss on Ignition (wt f)	Zinc (mg/kg)	Total Pb (mg/kg)	Hg (ng/g)	Pb Isotope Mass Ratio 204/206	Pb Isotope Mass Ratio 207/206	Pb Isotope Mass Ratio 208/206	Plutonium 239+240 (Bq/kg)
24	0.783	0.237	0.089	132.6	17.91					
25	0.798	0.216	0.083	137.1	17.00	54.21	0.05257	0.82234	2.0420	
26	0.789	0.228	0.092	125.4	15.78					
27	0.782	0.229	0.083	129.0	17.47					0.4567
28	0.783	0.231	0.091	135.7	17.49					
29	0.793	0.220	0.091	139.1	17.54					
30	0.780	0.231	0.089	138.9	19.18					
31	0.779	0.234	0.092	140.3	31.48					
32	0.788	0.228	0.088	188.7	18.04					
33	0.780	0.225	0.089	142.8	20.11					
34	0.767	0.256	0.082	135.9	17.80					
35	0.769	0.257	0.082	133.5	18.86	47.86				0.6357
36	0.771	0.247	0.097	142.5	9.78					
37	0.780	0.225	0.089	148.8	20.75					
38	0.784	0.221	0.090	141.5	20.05					
39	0.769	0.255	0.086	139.0	18.01					
40	0.779	0.244	0.090	146.6	21.72					
41	0.777	0.243	0.095	152.0	23.80					
42	0.765	0.256	0.090	144.6	23.33					
43	0.752	0.253	0.075	137.1	18.53					
44	0.744	0.273	0.095	147.8	23.91					
45	0.741	0.289	0.093	135.5	22.74	48.47				1.5336
46	0.742	0.283	0.099	148.1	16.64					
47	0.736	0.299	0.090	142.4	33.78					2.3042
48	0.737	0.296	0.095	149.9	10.86					2.8065
49	0.733	0.303	0.096	148.7	16.99					
50	0.717	0.323	0.093	149.1	23.56					
51	0.745	0.290	0.086	157.5	30.87					
52	0.506	0.700	0.086	141.2	23.95					3.0137
53	0.448	0.810	0.083	144.8	22.38					
54	0.426	0.873	0.085	155.6	26.18					
55	0.435	0.844	0.086	143.6	20.01	32.98				2.9067
56	0.422	0.859	0.087	144.8	20.61					
57	0.414	0.877	0.084	148.6	17.44					2.1027
58	0.406	0.905	0.084	156.0	16.98					
59	0.402	0.925	0.084	156.4	19.31					
60	0.398	0.958	0.081	147.5	22.81	24.81				
61	0.388	0.938	0.083	154.8						
62	0.396	0.916	0.076	147.5	21.96					
63	0.390	0.908	0.077	138.0	14.56					
64	0.396	0.881	0.079	148.7	20.91					
65	0.380	0.929	0.079	138.4	18.60	29.44	0.05281	0.82562	2.0477	0.5153
66	0.415	0.829	0.081	152.7	14.77					
67	0.421	0.849	0.085	146.5	15.48					
68	0.377	0.942	0.083	157.4	23.61					
69	0.385	0.951	0.078	170.1	16.63					

Lower Lake Mary

Depth (cm)	Moisture (wt f)	Bulk density (g/cc)	Loss on Ignition (wt f)	Zinc (mg/kg)	Total Pb (mg/kg)	Hg (ng/g)	Pb Isotope Mass Ratio 204/206	Pb Isotope Mass Ratio 207/206	Pb Isotope Mass Ratio 208/206	Plutonium 239+240 (Bq/kg)
0	0.516	0.657	0.142	285.6	58.80					
1	0.453	0.746	0.145	244.3	64.02					2.6314
2	0.452	0.796	0.141	269.8	58.23					

Depth (cm)	Moisture (wt f)	Bulk density (g/cc)	Loss on Ignition (wt f)	Zinc (mg/kg)	Total Pb (mg/kg)	Hg (ng/g)	Pb Isotope Mass Ratio 204/206	Pb Isotope Mass Ratio 207/206	Pb Isotope Mass Ratio 208/206	Plutonium 239+240 (Bq/kg)
3	0.467	0.741	0.142	271.9	38.44					
4	0.453	0.668	0.135	302.0	60.20					2.4824
5	0.432	0.796	0.127	251.2	64.87	81.91	0.05353	0.83499	2.0465	
6	0.398	0.892	0.135	254.2	54.12					
7	0.405	0.883	0.140	258.4	54.06					
8	0.414	0.791	0.139	251.2	54.04					
9	0.405	0.782	0.145	306.6	70.97					
10	0.392	0.679	0.146	263.0	54.80	86.65				2.9355
11	0.360	0.684	0.137	259.3	55.88					
12	0.361	0.718	0.132	253.8	62.24					
13	0.356	0.643	0.129	243.0	51.67					
14	0.374	0.701	0.140	253.7	57.34					
15	0.360	0.636	0.134	253.0	42.94	89.52				0.9386
16	0.413	0.801	0.135	243.2	50.46					
17	0.385	0.841	0.144	272.3	59.76					
18	0.445	0.776	0.129	236.1	51.21					
19	0.444	0.795	0.126	236.3	51.43					0.4608
20	0.433	0.830	0.129	234.4	53.78	86.20	0.05396	0.84055	2.0537	
21	0.439	0.771	0.125	224.9	44.21					
22	0.479	0.719	0.135	236.4	48.22					
23	0.456	0.776	0.142	256.7	47.70					
24	0.497	0.680	0.131	234.5	43.30					
25	0.454	0.777	0.132	253.8	43.52					

White Mountains**Lyman Lake**

Depth (cm)	Moisture (wt f)	Bulk density (g/cc)	Loss on Ignition (wt f)	Zinc (mg/kg)	Total Pb (mg/kg)	Hg (ng/g)	Pb Isotope Mass Ratio 204/206	Pb Isotope Mass Ratio 207/206	Pb Isotope Mass Ratio 208/206	Plutonium 239+240 (Bq/kg)
Surface Core										
0	0.745	0.219	0.094	97.4	29.26					
5	0.698	0.357	0.090	98.4	25.17					0.2857
10	0.685	0.362	0.090	104.9	28.70	36.18				
15	0.745	0.272	0.094	101.3	29.01					0.4350
20	0.746	0.289	0.096	118.7	28.67					
25	0.741	0.468	0.091	102.2	29.31					
30	0.723	0.304	0.098	109.4	30.43					0.4267
35	0.522	0.616	0.090	104.9	30.36					
40	0.729	0.308	0.092	130.5	31.83					
45	0.730	0.299	0.095	122.7	33.19					
50	0.733	0.290	0.099	153.0	30.74					0.4847
55	0.706	0.341	0.093	130.3	31.51					
60	0.708	0.336	0.095	98.5	27.17					
65	0.742	0.284	0.099	189.6	34.11					0.7682
70	0.669	0.375	0.090	117.3	26.50	34.69				
75	0.682	0.374	0.088	143.7	25.09					
80	0.596	0.503	0.087	126.3	23.58					
Livingstone Core										
56	0.727	0.308	0.095			23.40	0.05428	0.82988	2.0368	0.4686
86	0.726	0.304	0.115			22.10				1.3858
98	0.699	0.320	0.096			23.85				1.8206
111	0.590	0.492	0.085			17.42	0.05424	0.82260	2.0171	
121	0.571	0.548	0.100			21.42				0.5426
145	0.638	0.430	0.104			20.69				0.2908

Depth (cm)	Moisture (wt f)	Bulk density (g/cc)	Loss on Ignition (wt f)	Zinc (mg/kg)	Total Pb (mg/kg)	Hg (ng/g)	Pb Isotope Mass Ratio 204/206	Pb Isotope Mass Ratio 207/206	Pb Isotope Mass Ratio 208/206	Plutonium 239+240 (Bq/kg)
155	0.491	0.720	0.094							0.1315
166	0.618	0.454	0.092			20.53	0.05465	0.82230	2.0129	0.1126
180	0.562	0.587	0.094							0.2405
185	0.533	0.577	0.091							0.2216
210	0.548	0.571	0.097			21.12				0.1091
220	0.715	0.418	0.109							0.0819
223	0.646	0.453	0.134			27.37				0.0614
230	0.419	0.576	0.089			22.48	0.05408	0.82652	2.0348	0.0312
241	0.476	0.682	0.085			22.78				
249	0.435	0.846	0.082			21.49				0.1433
271	0.581	0.507	0.089			14.05				0.0443
284	0.519	0.642	0.092							0.0411
322	0.494	0.697	0.090				0.05367	0.81677	2.0123	0.0343
367	0.487	0.758	0.089				0.05444	0.82052	2.0131	
402	0.474	0.714	0.087			19.92	0.05431	0.81955	2.0095	
455	0.474	0.642	0.090				0.05414	0.81962	2.0094	

Carnero Lake

Depth (cm)	Moisture (wt f)	Bulk density (g/cc)	Loss on Ignition (wt f)	Zinc (mg/kg)	Total Pb (mg/kg)	Hg (ng/g)	Pb Isotope Mass Ratio 204/206	Pb Isotope Mass Ratio 207/206	Pb Isotope Mass Ratio 208/206	Plutonium 239+240 (Bq/kg)
1	0.955	0.047	0.313	207.0	51.36	95.27				
2	0.939	0.114	0.337	201.5	50.71					
3	0.936	0.121	0.330	199.5	51.30	102.79				
4	0.912	0.140	0.319	186.8	45.92					
5	0.913	0.152	0.294	171.5	44.45	90.29				1.3606
6	0.926	0.127	0.341	213.0	54.53					
7	0.914	0.167	0.286	169.2	42.45	118.03				
8	0.873	0.099	0.241	144.8	53.54					
9	0.852	0.151	0.204	220.9	29.89	108.74				
10	0.866	0.158	0.213	154.4	42.95					1.9885
11	0.863	0.119	0.238	152.2	43.41					
12	0.857	0.153	0.250	162.8	51.18	116.25				
13	0.862	0.145	0.256	174.5	53.54					4.3803
14	0.862	0.153	0.259	179.7	52.01					
15	0.865	0.128	0.262	173.2	47.59	139.74				4.5554
16	0.861	0.144	0.273	194.8	61.63					
17	0.848	0.140	0.266	178.6	55.41					
18	0.853	0.153	0.258	176.4	55.86	99.78				7.2956
19	0.832	0.177	0.252	165.3	49.90					
20	0.840	0.172	0.245	172.6	44.17					
21	0.840	0.166	0.237	156.5	48.42					1.2324
22	0.833	0.167	0.249	159.0	39.61	81.96				
23	0.824	0.172	0.223	140.3	29.60					1.9741
24	0.805	0.211	0.167	162.0	26.55					
25	0.802	0.209	0.206	172.2	32.32					0.3742
26	0.775	0.248	0.191	152.1	30.25					
27	0.794	0.238	0.181	155.4	25.77	80.15				
28	0.753	0.273	0.177	139.4	27.58					
29	0.747	0.261	0.171	146.2	27.58					
30	0.733	0.294	0.171	140.3	27.75					
31	0.697	0.333	0.164	148.6	28.37					
32	0.753	0.270	0.200	140.7	26.02					
33	0.677	0.368	0.143	119.4	23.81	53.47				

Depth (cm)	Moisture (wt f)	Bulk density (g/cc)	Loss on Ignition (wt f)	Zinc (mg/kg)	Total Pb (mg/kg)	Hg (ng/g)	Pb Isotope Mass Ratio 204/206	Pb Isotope Mass Ratio 207/206	Pb Isotope Mass Ratio 208/206	Plutonium 239+240 (Bq/kg)
34	0.622	0.458	0.139	113.9	22.09					
35	0.507	0.703	0.140	99.6	18.02					0.0882
36	0.402	0.890	0.106	94.2	19.62					
37	0.381	0.962	0.101	90.5	17.07					
38	0.463	0.776	0.143	98.9	19.04					
39	0.465	0.747	0.169	103.9	21.11					
40	0.431	0.791	0.149	100.9	20.95		0.05308	0.82794	2.0529	
41	0.353	1.028	0.092	94.0	18.97					
42	0.358	0.990	0.095	91.5	19.23					
43	0.354	1.044	0.092	92.1	16.39	30.70				
44	0.354	0.995	0.086	94.1	18.03					

Nelson Reservoir

Depth (cm)	Moisture (wt f)	Bulk density (g/cc)	Loss on Ignition (wt f)	Zinc (mg/kg)	Total Pb (mg/kg)	Hg (ng/g)	Pb Isotope Mass Ratio 204/206	Pb Isotope Mass Ratio 207/206	Pb Isotope Mass Ratio 208/206	Plutonium 239+240 (Bq/kg)
0	0.907	0.095	0.158	190.9	30.34					
1	0.902	0.101	0.149	252.0	29.36					
2	0.885	0.114	0.149	125.5	27.67	40.39				
3	0.874	0.130	0.154	119.2	27.71					
4	0.854	0.147	0.122	147.3	27.63		0.05406	0.83724	2.0639	
5	0.850	0.158	0.127	118.1	24.53					
6	0.838	0.172	0.116	139.9	18.54					
7	0.831	0.165	0.121	114.8	21.44					
8	0.819	0.187	0.123	148.8	25.51					
9	0.809	0.204	0.113	163.1	22.88					
10	0.832	0.178	0.103	137.2	25.32	35.63				0.8455
11	0.812	0.201	0.119	138.1	24.80					
12	0.818	0.192	0.115	186.8	24.78					
13	0.808	0.197	0.117	152.6	23.22					
14	0.819	0.198	0.111	154.8	26.69					
15	0.818	0.197	0.107	148.8	25.82					
16	0.820	0.195	0.123	164.2	28.13					
17	0.817	0.194	0.119	202.9	25.57					
18	0.809	0.201	0.114	198.5	23.94					
19	0.812	0.200	0.100	175.1	27.30					
20	0.810	0.203	0.106	119.7	26.98					0.3532
21	0.810	0.205	0.102	117.5	26.91					
22	0.806	0.204	0.098	171.7	22.87					
23	0.809	0.206	0.102	168.7	22.18					
24	0.790	0.228	0.105	212.3	26.06		0.05439	0.83700	2.0583	
25	0.786	0.220	0.106	145.1	27.23	34.42				0.3860
26	0.777	0.240	0.100	122.4	30.46					
27	0.775	0.245	0.102	164.2	30.24					
28	0.743	0.281	0.100	137.4	31.87					
29	0.770	0.252	0.099	131.9	25.86					
30	0.757	0.268	0.103	156.7	28.32					
31	0.717	0.320	0.091	108.3	30.64					
32	0.753	0.272	0.099	208.0	30.03					
33	0.739	0.292	0.092	100.4	28.63					
34	0.765	0.262	0.099	173.5	28.27					
35	0.779	0.235	0.106	107.5	27.29	35.76				0.6924
36	0.781	0.239	0.113	120.6	30.83					
37	0.768	0.251	0.104	137.7	31.27					

Depth (cm)	Moisture (wt f)	Bulk density (g/cc)	Loss on Ignition (wt f)	Zinc (mg/kg)	Total Pb (mg/kg)	Hg (ng/g)	Pb Isotope Mass Ratio 204/206	Pb Isotope Mass Ratio 207/206	Pb Isotope Mass Ratio 208/206	Plutonium 239+240 (Bq/kg)
38	0.760	0.269	0.112	117.9	30.49					
39	0.720	0.315	0.111	119.2	28.91					
40	0.748	0.270	0.111	173.9	27.54					0.6916
41	0.770	0.226	0.119	148.1	20.68					
42	0.758	0.260	0.108	109.7	30.59					
43	0.755	0.272	0.103	116.8	28.02					
44	0.752	0.273	0.103	112.7	25.65					
45	0.743	0.289	0.100	117.3	26.35	33.05				0.9532
46	0.719	0.310	0.090	135.6	31.70					
47	0.709	0.325	0.092	110.2	26.32					
48	0.692	0.350	0.089	113.1	27.28					
49	0.703	0.331	0.091	111.6	27.44					
50	0.696	0.327	0.100	111.8	25.69					0.6281
51	0.693	0.362	0.088	111.1	28.00					
52	0.696	0.345	0.093	109.8	25.36					
53	0.713	0.294	0.095	111.6	16.83					0.7852
54	0.711	0.312	0.090	108.0	27.81					
55	0.697	0.343	0.099	118.1	26.09	35.07				3.4599
56	0.674	0.371	0.097	119.7	31.73					
57	0.672	0.376	0.101	117.7	27.09					1.8123
58	0.629	0.440	0.102	124.7	23.67					
59	0.511	0.684	0.098	116.2	23.65					
60	0.426	0.855	0.097	111.5	27.59					0.8175
61	0.425	0.850	0.089	115.6	20.07					
62	0.412	0.895	0.093	123.8	30.20					
63	0.391	0.914	0.095	127.5	33.75					
64	0.392	0.926	0.093	113.4	27.23					
65	0.396	0.902	0.095	113.5	25.07	28.54	0.05456	0.84188	2.0747	0.2756
66	0.392	0.903	0.092	105.5	24.57	27.89				
67	0.390	0.901	0.098	116.4	25.66					
68	0.396	0.905	0.091	113.3	24.15	27.81				
69	0.380	0.974	0.092	148.9	21.36					

Mogollon Rim**Willow Springs Lake**

Depth (cm)	Moisture (wt f)	Bulk density (g/cc)	Loss on Ignition (wt f)	Zinc (mg/kg)	Total Pb (mg/kg)	Hg (ng/g)	Pb Isotope Mass Ratio 204/206	Pb Isotope Mass Ratio 207/206	Pb Isotope Mass Ratio 208/206	Plutonium 239+240 (Bq/kg)
0	0.824	0.182	0.183	165.9	127.63		0.05369	0.83704	2.0565	
1	0.654	0.426	0.123	73.6	48.80	127.11	0.05304	0.82749	2.0453	1.7872
2	0.531	0.627	0.108	111.4	35.31		0.05281	0.82455	2.0424	
3	0.235	0.842	0.101	60.3	33.29	55.06				
4	0.192	1.089	0.092	45.6	26.88					0.5307
5	0.235	1.178	0.081	46.7	23.60	24.62				
6	0.386	1.372	0.071	44.1	20.69					
7	0.320	1.075	0.115	79.5	30.83					0.3320
8	0.487	1.189	0.097	74.2	25.07	26.07				
9	0.316	1.135	0.092	67.0	24.65					
10	0.293	1.240	0.086	66.9	29.01					0.3961
11	0.256	1.309	0.085	57.4	23.33					
12	0.252	1.336	0.082	63.5	13.86	21.13				
13	0.258	1.275	0.086	61.0	32.83					0.2591
14	0.271	1.208	0.086	60.6	28.06					
15	0.304	1.167	0.078	58.6	29.60	23.29				

Depth (cm)	Moisture (wt f)	Bulk density (g/cc)	Loss on Ignition (wt f)	Zinc (mg/kg)	Total Pb (mg/kg)	Hg (ng/g)	Pb Isotope Mass Ratio 204/206	Pb Isotope Mass Ratio 207/206	Pb Isotope Mass Ratio 208/206	Plutonium 239+240 (Bq/kg)
16	0.249	1.304	0.077	54.9	25.77					
17	0.279	1.244	0.076	58.5	28.76					
18	0.287	1.210	0.083	63.8	27.23					0.1551
19	0.285	1.215	0.073	56.0	24.73					
20	0.282	1.229	0.078	64.2	26.54	23.15	0.05304	0.82749	2.0453	
21	0.285	1.226	0.074	55.8	24.18					
22	0.281	1.260	0.078	52.5	24.30					0.1293
23	0.296	1.188	0.083	70.8	30.45					
24	0.272	1.229	0.109	90.4	27.92					
25	0.276	1.305	0.079	63.9	24.58	26.55				
26	0.280	1.251	0.080	60.1	21.39					
27	0.289	1.217	0.080	70.0	26.57					0.1400
28	0.295	1.213	0.087	59.8	28.14					
29	0.287	1.202	0.082	77.3	30.06					
30	0.274	1.274	0.078	93.3	27.82					
31	0.261	1.305	0.080	70.1	13.21					
32	0.272	1.216	0.086	72.5	15.39					
33	0.286	1.197	0.087	78.1	14.98					0.0711
34	0.296	1.149	0.080	71.2	15.19					
35	0.288	1.187	0.082	71.8	15.40	23.83	0.05281	0.82455	2.0424	
36	0.274	1.268	0.083	87.3	15.18					
37	0.281	1.211	0.084	75.6	15.49					0.0307
38	0.285	1.204	0.079	83.5	17.32					

Stoneman Lake

Depth (cm)	Moisture (wt f)	Bulk density (g/cc)	Loss on Ignition (wt f)	Zinc (mg/kg)	Total Pb (mg/kg)	Hg (ng/g)	Pb Isotope Mass Ratio 204/206	Pb Isotope Mass Ratio 207/206	Pb Isotope Mass Ratio 208/206	Plutonium 239+240 (Bq/kg)
0	0.862		0.427	598.2	52.56					
1	0.579		0.138	144.5	30.28					
2	0.388		0.110	130.4	31.32					1.1171
3	0.262		0.105	139.1	31.89		0.05643	0.87819	2.1198	
4	0.279		0.107	144.5	35.97					
5	0.133		0.108	128.5	35.32					0.3547
6	0.175		0.107	138.1	29.26					
7	0.154		0.108	135.8	30.60					
8	0.206		0.099	129.1	30.52					0.5799
9	0.179		0.102	120.0	27.87					
10	0.125		0.102	132.1	30.44					
11	0.246		0.099	128.7	25.62					
12	0.222		0.098	135.4	29.82					
13	0.179		0.101	121.3	27.56					
14	0.242		0.101	132.2	27.56					
15	0.126		0.103	130.2	29.34					0.3501
16	0.122		0.102	128.2	28.78					
17	0.146		0.102	133.3	28.02					
18	0.116		0.104	133.7	26.57					0.5490
19	0.126		0.103	131.1	24.26					
20	0.144		0.105	127.1	27.05		0.05356	0.83558	2.0613	
21	0.185		0.101	277.1	25.36					

Central Arizona**Alamo Reservoir**

Depth (cm)	Moisture (wt f)	Bulk density (g/cc)	Loss on Ignition (wt f)	Zinc (mg/kg)	Total Pb (mg/kg)	Hg (ng/g)	Pb Isotope Mass Ratio 204/206	Pb Isotope Mass Ratio 207/206	Pb Isotope Mass Ratio 208/206	Plutonium 239+240 (Bq/kg)
Depth (cm)	Moisture (wt f)	Bulk density (g/cc)	Loss on Ignition (wt f)	Zinc (mg/kg)	Total Pb (mg/kg)	Hg (ng/g)	Pb Isotope Mass Ratio 204/206	Pb Isotope Mass Ratio 207/206	Pb Isotope Mass Ratio 208/206	Plutonium 239+240 (Bq/kg)
Surface Core										
0	0.776	0.241	0.103	208.9	54.59					
5	0.725	0.310	0.091	192.5	34.81					
10	0.512	0.644	0.075	143.1	34.46	59.83	0.05214	0.81627	2.0279	
15	0.359	1.238	0.038	173.5	34.70					
20	0.497	0.701	0.079	157.7	37.36					
25	0.472	0.718	0.076	249.9	52.95					
30	0.748	0.278	0.107	223.7	54.76	78.91				
35	0.562	0.557	0.086	206.2	49.44					
40	0.528	0.602	0.086	182.6	46.91					
45	0.504	0.657	0.083	206.0	44.10					
50	0.620	0.446	0.073	162.9	39.58					
53	0.594	0.505	0.078							
Livingstone Core										
38	0.487	0.690	0.090			46.75	0.05341	0.81879	2.0076	
55						56.54				
85	0.604	0.458	0.092			51.25				
100						60.98				
125	0.550	0.622	0.087			60.57				
147	0.578	0.534	0.094			61.92	0.05296	0.79914	1.9745	
174						66.34				
202	0.553	0.542	0.111			61.61	0.05116	0.78148	1.9519	
242	0.569	0.518	0.089			55.13				
257						63.59				
272	0.591	0.636	0.101			68.20				
297						81.44				
319	0.391	0.906	0.082			53.53				
329	0.573	0.542	0.111			64.12				
347						69.69				
379	0.467	0.768	0.096			53.96				
421						70.15				
435						101.60				
441	0.455	0.804	0.112							
442						78.78				

Date	Lake	Elevation (ft)	GPS Position	Corer	Core #	Drive #	Water Depth (cm)	Start Depth (cm)	Driven (cm)	Recovered (cm)	Notes
1-May-04	Lake Mary	7297	N35°04.794', W111°32.007'	Anderson	1	x	680	0	x	23	Lost ~15cm out the bottom at natural change in sediment
				Anderson	2	x	670	0	x	50	
				Livingston	3	1	670	20	57	54.5	
					3	2	x	x	38	38	
27-May-04	Stehr Lake	3705	N34°21.853', W111°40.143'	Anderson	1	x	565	0	x	47.5	
				Livingston	2	1	561	29	100	71	
				Livingston	3	1	560	29	104	59	
				Livingston	3	2	x	x	82	82	
29-May-04	Kinnickinick Lake	7037	N34°53.904', W111°18.376'	Anderson	1	x	670	0	x		
11-Jul-04	Soldiers Lake	????	N34°47.784', W111°14.045'	Anderson	SC1	x	430	0	x		
				Livingston	1	1	492	30	49.5	45	compressed b/t 16-20cm
				Livingston	1	2	x	x	15	15	
11-Jul-04	Long Lake										
12-Jul-04	Lower Lake Mary										
13-Jul-04	Ashurst Lake	????	N35°01.256', W111°24.220'	Anderson	SC1	x	238	0	x	40.5	transition to darker sediment at ~20cm
	Nelson		N34°04.558',								filamentous algae suspended in water column, abrupt
7-Aug-04	Reservoir	7578	N34°22.250', W109°11.634'	Anderson	SC1	x	515	0	x	69	change from dark gyttja to lighter at 57cm
7-Aug-04	Lyman Lake	5964	N34°22.251', W109°22.913'	Anderson	SC1	x	360	0	x		water very turbid
			N34°22.251', W109°22.914'	Livingston	1	1	359	20	100	104	extra 4cm was sticking out of the end of the corer
				Livingston	1	2	x	x	100	100	extra 2cm was sticking out of the end of the corer
				Livingston	1	3	x	x	100	99	
				Livingston	1	4	x	x	100	93	
				Livingston	1	5	x	x	37	36	extra 3cm was sticking out of the end of the corer
8-Aug-04	Carnero Lake	9003	N34°07.010', W109°31.708'	Anderson	SC1	x	210	0	x	45	38-45cm is pink clay
9-Aug-04	Willow Springs	7534	N34°18.851', W110°52.549'				1860				no core recovered
17-Aug-04	Alamo Lake	1060	N34°14.701', W113°35.312'	Foust	SC1	x	1700	0	x		0-3cm dark, organic; 3-31cm reddish, gray, light; 31-41 dark; 54 41-45 light; 45-59 dark; 49-54 dark
				Livingston	1	1	1680	15	100		lost ~4cm out the bottom; sediment degassed on the way up;
				Livingston	1	2	x	x	100		89 air pockets evident in the sediment column
											89 lost ~4cm out the bottom
											corer got stuck on casing joint, could not push drive farther;
											storm rolls in w/strong wind, moved from initial coring
				Livingston	1	3	x	x	74	76	location
18-Aug-04			N34°14.575', W113°35.257'	Livingston	2	1	1706	20	100	106	lost ~8cm out the bottom, but sediment degassed on the way
				Livingston	2	2	x	x	77		up and expanded
				Livingston	2	3	x	x	100	103.5	80 corer got stuck on casing; lost ~4cm out the bottom
											lost ~4cm out the bottom, 52-57cm got compressed during
				Livingston	2	4	x	x	96	77	extrusion
				Livingston	2	5	x	x	65	53	lost ~1cm out the bottom
19-Aug-04	Willow Springs	7526	N34°18.822', W110°52.577'	Foust	SC1	x	1910	0	x	24	
											sediment is dark, organic, sandy with fibrous structures-
											possibly roots, but there is no branching like typical root
											structure. Pine needles present. Sediment is dry toward the
			N34°18.860', W110°52.594'	Foust	SC2	x	1770	0	x	39	base of the core and crumbly.*